Rose-Hulman Institute of Technology
Rose-Hulman Scholar

Graduate Theses - Physics and Optical Engineering | Graduate Theses

Summer 8-2015

Increasing the Sensitivity of the Michelson Interferometer through Multiple Reflection

Woonghee Youn

Follow this and additional works at: http://scholar.rose-hulman.edu/optics_grad_theses

Part of the Engineering Commons, and the Optics Commons

Recommended Citation

Youn, Woonghee, "Increasing the Sensitivity of the Michelson Interferometer through Multiple Reflection" (2015). *Graduate Theses - Physics and Optical Engineering.* Paper 7.

This Thesis is brought to you for free and open access by the Graduate Theses at Rose-Hulman Scholar. It has been accepted for inclusion in Graduate Theses - Physics and Optical Engineering by an authorized administrator of Rose-Hulman Scholar. For more information, please contact bernier@rose-hulman.edu.

Increasing the Sensitivity of the Michelson Interferometer through Multiple Reflection

A Thesis

Submitted to the Faculty

of

Rose-Hulman Institute of Technology

by

Woonghee Youn

In Partial Fulfillment of the Requirements for the Degree

of

Master of Science in Optical Engineering

August 2015

© 2015 Woonghee Youn

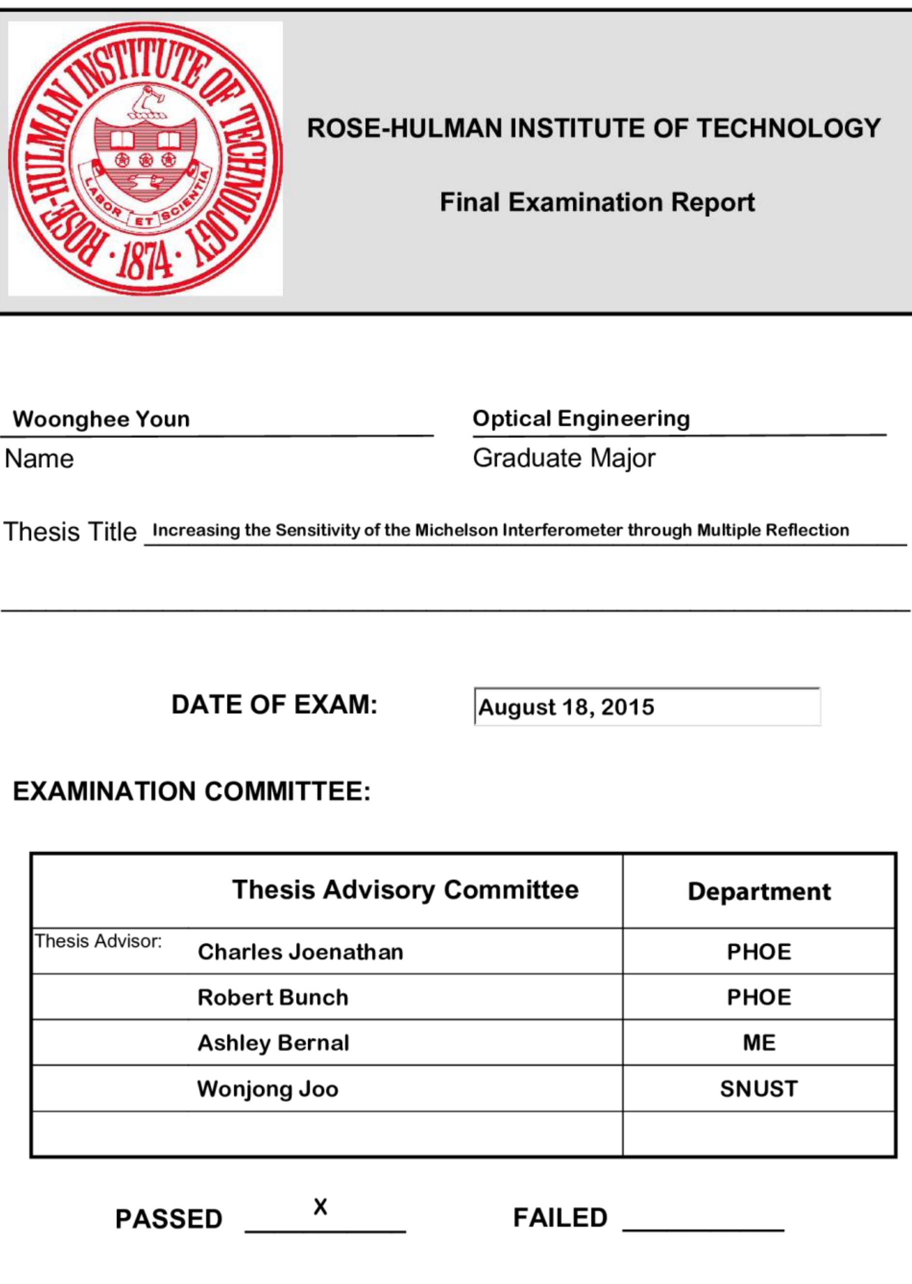

ROSE-HULMAN INSTITUTE OF TECHNOLOGY

Final Examination Report

Woonghee Youn
Name

Optical Engineering
Graduate Major

Thesis Title **Increasing the Sensitivity of the Michelson Interferometer through Multiple Reflection**

DATE OF EXAM: August 18, 2015

EXAMINATION COMMITTEE:

	Thesis Advisory Committee	Department
Thesis Advisor:	Charles Joenathan	PHOE
	Robert Bunch	PHOE
	Ashley Bernal	ME
	Wonjong Joo	SNUST

PASSED X **FAILED** ____

ABSTRACT

Youn, Woonghee

M.S.O.E

Rose-Hulman Institute of Technology

August 2015

Increase a sensitivity of the Michelson interferometer through the multiple reflection

Dr. Charles Joenathan

Michelson interferometry has been one of the most famous and popular optical interference system for analyzing optical components and measuring optical metrology properties. Typical Michelson interferometer can measure object displacement with wavefront shapes to one half of the laser wavelength. As testing components and devices size reduce to micro and nano dimension, Michelson interferometer sensitivity is not suitable. The purpose of this study is to design and develop the Michelson interferometer using the concept of multiple reflections. This thesis proposes a new and novel design for a multiple reflection interferometer, where the number of reflections does not affect the quality of the interference. Theoretically we show that more than 1000 reflections can be achieved. Experimental results of greater than 100 reflections are presented in this thesis.

ACKNOWLEDGMENT

I would have never been able to finish my study without my family, mother, father and sister.

First and foremost I really want to express my sincere gratitude to my advisor Prof. Charles Joenathan, chair of RHIT Physics and Optical Engineering Department, for endless support of my study and life in Rose-Hulman Institute of Technology. He has been supportive since I arrived school and he encouraged me when I had tough time. His guidance helped me in all the time of research and study. I could not forget his advises and assists.

I would like to thank my thesis committees: Prof. Ashley Bernal, Prof. Robert Bunch, Prof. Kim Sungdong and Prof. Joo Wonjong for their guidance, caring and encouragements. My sincere thanks also goes to Prof. Sarah Eunkyung Kim, who advised me when I was in Korea, and Prof. Michael McInerney. Prof. Michael McInerney helped me and my friends when we settled down in Terre Haute. And I would like to show appreciation to my friends; Benjamin, Yonghee, Wanseok, Junyeob, Yeohun, Yanzeng and Heesoo. They were always willing to help and give their best suggestions.

사랑하는 어머니, 아버지, 동생 세희, 그리고 절 친 자식처럼 아껴주시는 이모, 이모부께 감사 드립니다.

My sense of gratitude to one and all, who helped me directly or indirectly.

TABLE OF CONTENTS

LIST OF FIGURE V

LIST OF TABLE VIII

1. Introduction 1

2. Theory and Design 3

2.1 Background Theory and Design 3

2.1.1 Michelson interferometer 3

2.1.2 Superposition of waves 6

2.1.3 Sensitivity of the Michelson interferometer 9

2.2 Multiple reflection Michelson interferometer in one arm 11

3. Design Concept for dual arm Multi-Reflection Interferometer 14

3.1 Disadvantage of the one arm multiple reflection interferometer 14

3.2 Relation between incident beam angle and wedge shape mirror angle 15

3.3 Sensitivity of the multiple reflection interferometer 16

3.3.1 Displacement sensitivity 17

3.3.2 Effect of incident angle 20

3.4 Concept design for dual arm multi-reflection interferometer 21

4. Experiment 23

4.1 Experimental set-up 27

4.2 Experimental procedures 29
4.2.1 Displacement sensitivity difference by incidence angle 29
4.2.2 Displacement sensitivity with multiple reflection 32
5. Result 34
5.1 Relationship between incidence angle and wedge shape mirror angle 34
5.2 Displacement sensitivity difference by incidence angle 36
5.3 Displacement sensitivity of multiple reflection 38
6. Conclusion 48
7. Future Work 49
LIST OF REFERENCES 50
APPENDIX A 53

LIST OF FIGURE

Figure 1 **Schematic diagram of the Michelson interferometer** 4

Figure 2 **The beam travelling in the beam splitter and compensator plate** 5

Figure 3 **Fringe pattern when the optical path length of two arms are (a) equal and (b) different** 6

Figure 4 **The result of (a) constructive interference and (b) destructive interference** 7

Figure 5 **Schematic diagram of the optical path difference of the Michelson interferometer. M1 and M2 are mirrors, S1 and S2 are virtual source positions, and d is a distance of M2 from M1.** 10

Figure 6 **Schematic diagram of the multiple reflection interferometer** 12

Figure 7 **Beam incidents diagram in the two-mirror wedge** 15

Figure 8 **The motion of beam at the two-mirror wedge when the mirror is displaced by a distance ‘d’. [3]** 18

Figure 9 **Optical path change when incidence angle is (a) small and (b) large between two mirrors. The solid line shows original beam moving path and dash-line shows a beam moving path after displacement of the mirror M2 [5]** 20

Figure 10 **Schematic diagram of Dual Reflection Interferometer** 22

Figure 11 Location of gears, mirrors, and rotational stage in schematic view; Mirror 3 and 1 are fixed mirrors and these mirrors are connected by a magnet based stage. Mirror 2 and 4 are mounted on gears. The gears are meshed at a distance 'a' (a is 3 inches). The rotating tab is able to rotate the stage in 0.04 degree increments.24

Figure 12 Schematic diagram of 4 mirrors in the dual arm multiple reflection interferometer after rotating the gear.........25

Figure 13 Modified multiple reflection Michelson interferometer........26

Figure 14 (a) Two 3 inch gears on the magnet base and (b) PZT mirror and normal mirror set on the gears........28

Figure 15 Picture of the beam reflection through the wedge shape mirror arms. Outside mirrors were fixed and inside mirrors were mounted on the 3 inch gear and rotation stage.........28

Figure 16 A reflection number calculating program according to mirror and incident angel. The wedge shape angle and beam incident angle are 45 degree........31

Figure 17 Diagram of the beam reflection number with different incident angle and wedge shape mirror angle........35

Figure 18 The detector signal for the fringe pattern change when the incidence angle and wedge-mirror angle are one degree. The x-axis is the displacement of the mirror and y-axis is the signal from the photo detector........37

Figure 19 The detector signal for the fringe pattern change when the incidence angle and wedge-mirror angle are 20 degrees.....37
Figure 20 Typical Michelson interferometer (1 reflection).....38
Figure 21 Multiple reflection interferometer (2 reflections).....39
Figure 22 Multiple reflection interferometer (12 reflections).....40
Figure 23 Multiple reflection interferometer (25 reflections).....40
Figure 24 Multiple reflection interferometer (50 reflections).....41
Figure 25 Multiple reflection interferometer (70 reflections).....41
Figure 26 Multiple reflection interferometer (110 reflections).....42
Figure 27 Average Displacement Sensitivity according to reflection number.....46
Figure 28 Displacement sensitivity error depending on reflection number in distance (nm) and percentage.....46
Figure 29 The simulation of beam reflection in the roof top mirror design with the same scale of the wedge shape.....49

LIST OF TABLE

Table 1 Displacement sensitivity according to PZT mirror displacement of 500, 1000 and 2000 nm and its average result.................................. 43

Table 2 Displacement sensitivity of multiple reflection interferometer and its error to compare with equation results. The equation (27) is compared 44

1. INTRODUCTION

Interferometry is a measurement technique where two light waves generated from one source are superposed. The resultant intensity at any point depends on whether they reinforce or cancel each other. Optical interferometry has been used as a laboratory technique for almost a hundred years [1, 2]. This technique is applied to many fields of optical metrology, fiber optics, many types of topology measurements, seismology, particle and plasma physics, medical analysis systems, molecular biology and mechanical stress and strain measurements. Interferometer measurement systems are used extensively in industrial application and could be used as a powerful tool for measuring displacements by taking advantage of lights ability to interfere with itself.

Among the interferometer systems used for practical applications, it has been suggested that the Michelson interferometer is the most common optical measuring system. This study proposes an advanced version of a Michelson interferometer which is named 'Dual Arm Multi-Reflection Interferometer'. This proposed system increases the sensitivity of the interferometry. The sensitivity of a standard Michelson interferometer is $\lambda/2$, where λ is the wavelength of the laser being used. However, with multiple reflection it has been shown that the sensitivity can be improved to over $\lambda/100$. The sensitivity is not only based on the number of reflections but also in the mirror assembly. There are some studies to obtain high resolution in the two beam interferometer, such as a multiple

total internal reflection interferometer, which was used to measure the changes in the displacement in the order of micro to nano magnitude range [5-8]. Chandra et al. introduced multiple reflections in one arm of the Michelson interferometer and showed that the sensitivity can be increased to $\lambda/72$ [3]. Further, a prism assembly was used to apply multiple reflections for the measurement of small vibrations [4]. Also, this multiple reflection interferometer can be made into a more compact design. Recently multiple reflection interferometry has been used to study noise levels and the linearity between the number of reflections and the improvement in resolution. Because the multiple reflection interferometer is composed of only a one arm multiple reflection (see fig. 6), this system has two disadvantages. First, the multiple reflections increase the optical path length in one arm thereby the path length difference between the two arms can easily exceed the coherence length of the laser thereby the visibility of the fringes will decrease to zero. In this study, a method of generating identical multiple reflections in both the arms of the interferometer is proposed. This thesis discusses the theoretical aspect of the multiple reflections and a novel mechanical design to generate identical multiple reflections in both the arms. Both the experimental design and experimental results are presented.

2. THEORY AND DESIGN

2.1 Background Theory and Design

In this chapter the fundamentals of wave superposition and the sensitivity in a Michelson interferometer are discussed.

2.1.1 Michelson interferometer

An optical arrangement to have wave interference was introduced by Albert Abraham Michelson in 1887. This amplitude division interferometer has played a significant role in the optical interferometer field, and the schematic arrangement is shown in fig. 1. This method is simple and has been used in a Fourier transform spectrometer, modified to a Twyman-Green interferometer setup and to a laser unequal path interferometer. In addition, multiple reflections have also been introduced in the Michelson interferometer to increase its sensitivity [16].

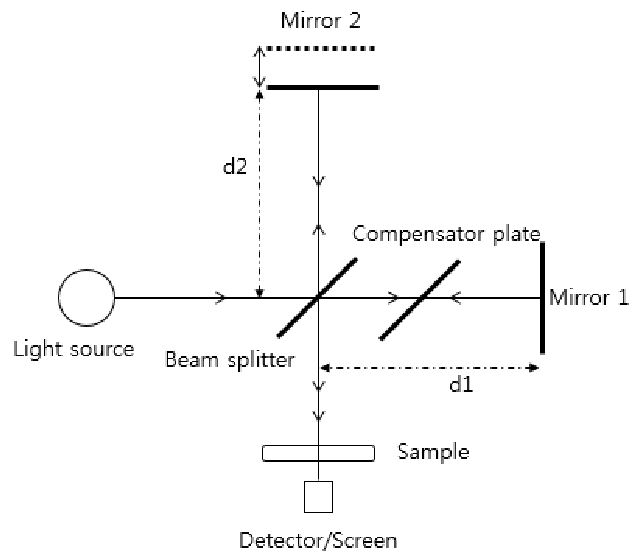

Figure 1 Schematic diagram of the Michelson interferometer

The arrangement of a Michelson interferometer consists of two mirrors, a single light source (monochromatic or quasi monochromatic), and a beam splitter as shown in fig. 1. The interferometric arrangement generates two coherent waves from a single monochromatic or quasi monochromatic light source. The beam is passed through a 50/50 beam splitter which divides the incident beam into two beams of equal amplitude. One beam goes to Mirror 1 and the other goes to Mirror 2. After reflection, the two split beams retrace their path and recombine at the beam splitter.

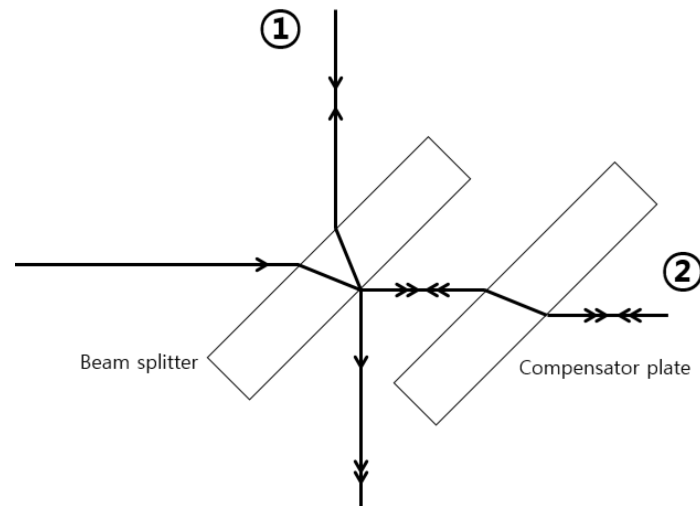

Figure 2 The beam travelling in the beam splitter and compensator plate

If the optical path lengths between the two beams are the same, the beams would arrive with the same phase and interfere constructively. For the Michelson interferometer there is a slight complication. The beam traveling toward Mirror 2 is in effect reflected inside the beam splitter, so it requires a compensator plate to account for dispersion if a non-monochromatic or white light source is used. Fig. 2 shows the schematic arrangement of the beam splitter and the compensator assembly. Note that beam 1 goes through the beam splitter twice and beam 2 will traverse the compensator twice, this compensates for the dispersion effects on beam 1. Mirror 1 or 2 is mechanically connected to some external device that allows the mirror to move. According to the movement of the mirror, the interference between the two beams will change from being either bright to dark or vice versa. When both the arms of the optical path length in the

Michelson interferometer are matched, a fringe is detected as shown fig. 3 (a). This is the only time that one dark and one bright fringe appear in the entire field of the wavefront. If one of the mirrors is moved such that the optical path lengths are different this causes, the number of fringes to increase as shown fig. 3 (b).

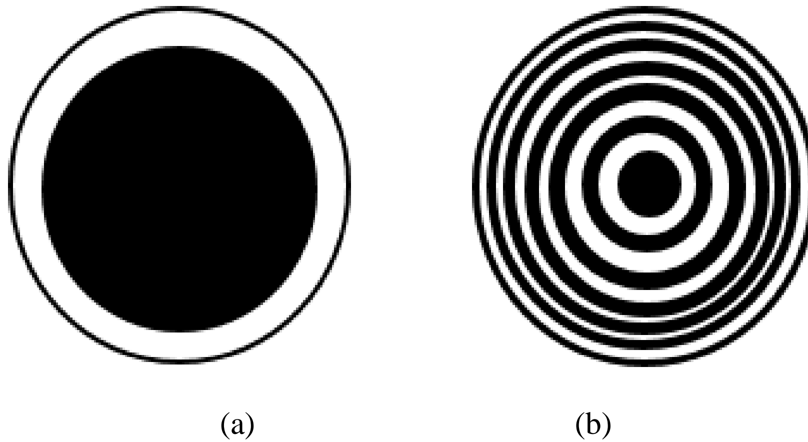

(a) (b)

Figure 3 Fringe pattern when the optical path length of two arms are (a) equal and (b) different

2.1.2 Superposition of waves

Michelson interferometer is an application of wave superposition. When two waves of same frequency and wavelength travel through the same medium, their amplitude can be added or canceled [11-13]. Fig. 4 shows constructive and destructive interference of a transverse wave.

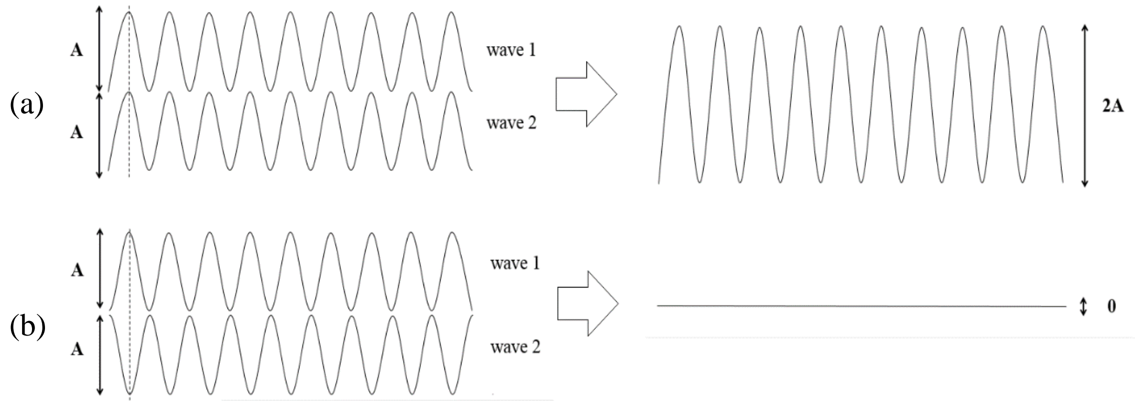

Figure 4 The result of (a) constructive interference and (b) destructive interference

There are several methods to combine two waves. In this paper, the superposition of waves is described by the traditional algebraic method.

The differential wave equation can be written in the form

$$E_q(\mathrm{x},\mathrm{t}) = E_{01}\sin[wt - (kx + \varepsilon)] \tag{1}$$

where E_{01} is the amplitude of the harmonic disturbance propagation along the positive x-axis, 'ω' is the angular frequency, 't' is the time, 'k' is the propagation number, and 'ε' is the initial phase. To separate the space and time domain parts of the phase, the space component of the phase can be expressed as

$$\alpha_1(\mathrm{x},\varepsilon) = -(kx + \varepsilon)$$

so that equation (1) becomes

$$\mathrm{E}_1(\mathrm{x},\mathrm{t}) = E_{01}\sin[wt + \alpha_1(x,\varepsilon)] \tag{2}$$

The equation for the second wave is

$$E_2 = E_{02}\sin[(wt + \alpha_2(x, \varepsilon)] \tag{3}$$

When these two waves superpose, the resultant disturbance is expressed as the sum of the two waves and is

$$E_T = E_1 + E_2 \tag{3}$$

Subtracting for E_1 and E_2, E_T becomes

$$E_T = E_{01}\sin(wt + \alpha_1) + E_{02}\sin(wt + \alpha_2) \tag{4}$$

Since the intensity is the square of the amplitude, equation (4) can be reduced to

$$E_0^2 = E_{01}^2 + E_{02}^2 + 2E_{01}E_{02}\cos(\alpha_2 - \alpha_1) \tag{5}$$

and tan α can be expressed as

$$\tan\alpha = \frac{E_{01}\sin\alpha_1 + E_{02}\sin\alpha_2}{E_{01}\cos\alpha_1 + E_{02}\cos\alpha_2} \tag{6}$$

The total disturbance can now be expressed as

$$E = E_0\cos\alpha\sin wt + E_0\sin\alpha\cos wt \tag{7}$$

or

$$E = E_0\sin(wt + \alpha) \tag{8}$$

This demonstrates that superposed two waves E_1 and E_2 become a single disturbance.

2.1.3 Sensitivity of the Michelson interferometer

When two waves are superposed, two types of interference are detected: constructive and destructive (see fig. 4). The working theory of the Michelson interferometer is that a single fringe pattern shows up on the screen or detector. If the peak and valley of the two superposing waves match exactly, then a maximum is obtained. Alternatively, if the peak (and valley) of two waves do not match and are off by 180 degrees, then the resultant amplitude will be a minimum.

The amplitude for two superposed waves in the Michelson interferometer is shown as equation (5). If two waves have the same phase, equation (5) can be changed to

$$E_0^2 = E_{01}^2 + E_{02}^2 + 2\mathrm{E}_{01}\mathrm{E}_{02} \qquad \{\alpha_2 = \alpha_1\} \tag{9}$$

If two waves has 180 degrees different phase, equation (5) can be

$$E_0^2 = E_{01}^2 + E_{02}^2 - 2\mathrm{E}_{01}\mathrm{E}_{02} \qquad \{\alpha_2 = \alpha_1 + \pi\} \tag{10}$$

The result of equation (9) and (10) shows a maximum and minimum value respectively. The π shows the phase difference which is generated by the mirror movement. The intensity of the superposing beams fluctuates between bright and dark as the mirror is displaced in the line of the beam. In the Michelson interferometer, the displacement distance of the optical path, that causes the fringe pattern intensity to cycle from a maximum to a minimum, is called the sensitivity. In the equation (10), the phase cycle is π and in terms of distance it is $\lambda/2$, where λ is the laser wavelength. Thus, the sensitivity of the Michelson interferometer is

$$\text{Sensitivity:} \qquad S = \frac{\lambda}{2} \qquad (11)$$

2.1.3.1 Optical path difference

In the Michelson interferometer, mirror 2 (fig. 5) moves back and forth to introduce a path difference. For every λ/2 optical path difference, the amplitude of the resulting superposed wave will change. Fig. 5 demonstrates how the optical path difference is introduced by mirror displacement ‘d’.

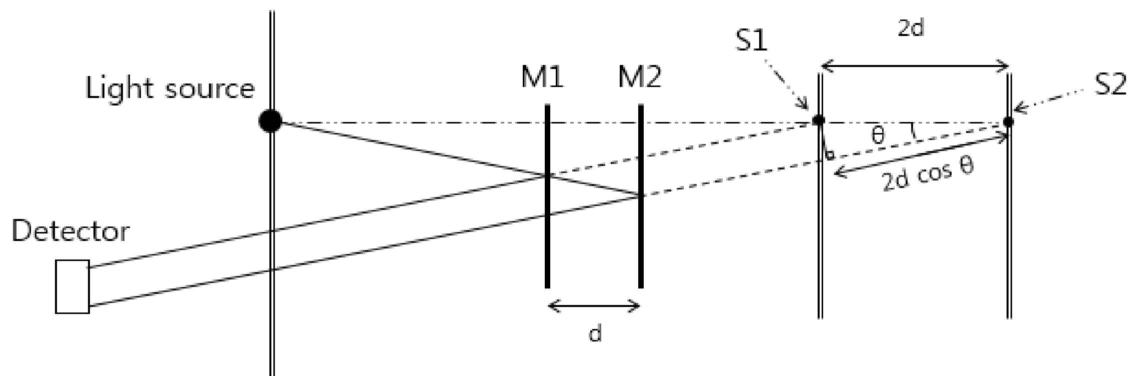

Figure 5 Schematic diagram of the optical path difference of the Michelson interferometer. M1 and M2 are mirrors, S1 and S2 are virtual source positions, and d is a distance of M2 from M1.

If the light source to detector movement is ‘d’, the total path difference is ‘2d’. The total optical path difference ‘δ’ caused by the beam diverging can be expressed as

$$\delta = 2\,\mathrm{d}\cos\theta \tag{12}$$

where ‘θ’ is the angle, the beam makes with reflection to the normal. In the displacement sensitivity of the Michelson interferometer, d is

$$\frac{\lambda}{2} = 2\,\mathrm{d}\cos\theta \tag{13}$$

$$\mathrm{d} = \mathrm{D} = \frac{\lambda}{4\cos\theta} \tag{14}$$

Here θ is zero if the beams are collimated and only one fringe is observed.

$$\mathrm{D} = \frac{\lambda}{4} \tag{15}$$

Therefore in a Michelson interferometer, the minimum displacement that can be measured is λ/4.

2.2 Multiple reflection Michelson interferometer in one arm

It was shown earlier that Michelson interferometer can be used to measure displacements greater than λ/4. However, the Michelson interferometer cannot measure below half the wavelength of light. So, a multiple reflection interferometer in one arm was developed to overcome this limitation [5, 9, 10]. In order to create multiple beam reflections, another mirror is added facing the existing mirror. As it is shown in fig. 6, another mirror (mirror 2) is added in front of mirror 1, creating a wedge angle. The beam in arm 1 goes through multiple reflections between mirror 1 and mirror 2.

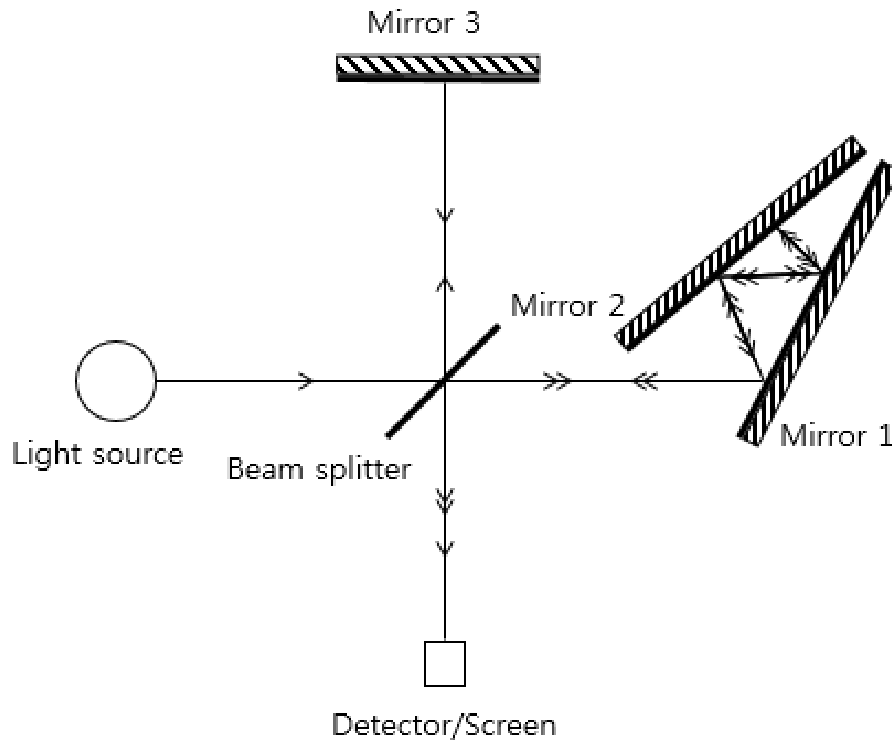

Figure 6 Schematic diagram of the multiple reflection interferometer

The beam undergoes a series of reflections between mirror 1 and mirror 2 until the beam hits one of the mirrors with a zero degree incidence angle. After the incidence angle reaches zero degree, the beam returns back to the beam splitter with the same path. Then, this multiple reflected beam combines with the beam from mirror 3 at the plane of the beam splitter as shown in fig. 6. The sensitivity is now determined by the number of reflections between mirror 1 and 2. If mirror 1 is displaced, the number of cycles of

maximum to minimum will be amplitude by the number of reflections when compared to the conventional Michelson interferometer.

3. DESIGN CONCEPT FOR DUAL ARM MULTI-REFLECTION INTERFEROMETER

In chapter 2, the Michelson interferometer principle, superposition theory, sensitivity of the system and theory of the multiple reflection interferometer was discussed. In this chapter, we discuss a method to maintain high visibility independent of the number of reflections called the “Dual Arm Multi-Reflection Interferometer”.

3.1 Disadvantage of the one arm multiple reflection interferometer

The conventional multiple reflection interferometer is an improved version of the Michelson interferometer, and its value for practical use is also increased because of the increase in sensitivity. However, this improvement has one disadvantage because the optical path difference between the two beams can be large for large numbers of reflection. The laser beam normally has a finite coherence length that can vary from a few nano-meters to several meters, and this depends on the type of the laser. A typical laser beam frequency spectrum consist of several narrow frequency ranges that contain most of the energy, and these are separated by much larger regions [14,15]. Thus the combined spectrum is broad consisting of a range of frequencies, thereby limiting the coherence length. The electron transitions generate light which has a duration on the order of 10^{-8} to 10^{-9} seconds. This emitted light can be affected by thermal motion and

collisions of atoms. So, the effect of all these mechanisms broadens the bandwidth of laser frequency rather than having one single frequency. The coherence length and time are components of this bandwidth. The coherence length in the frequency spectrum follows a sine curve form so that its phase can be predicted reliably [16].

If the optical path length difference is longer than the coherence length of the laser in the interferometer, the visibility of the fringe becomes zero. The one arm multiple reflection interferometer system has this disadvantage where the path difference could easily exceed the coherence length.

3.2 Relation between incident beam angle and wedge shape mirror angle

The incident beam angle and the angle of two wedge shape mirrors need to be calculated so that the reflected beam retraces its initial incidence path. Fig. 7 shows a schematic diagram of beam reflection in the two-mirror wedge.

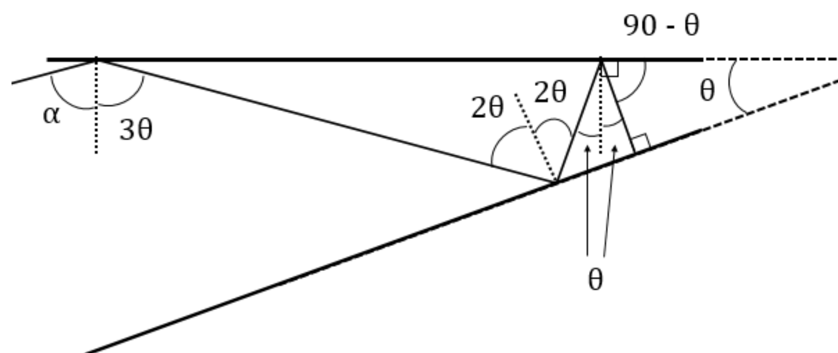

Figure 7 Beam incidents diagram in the two-mirror wedge

The condition for the reflected beam to come back on itself after the reflection is that the incident beam angle has to become 90 degrees. Suppose that the total reflection number is 'N', the angle between two mirrors is 'θ', and the initial incidence angle is 'α', the final incident beam angle must be normal (zero degree) to the mirror in order to retrace its initial incident beam path. If the final reflection beam's (N times reflections) angle is 90 degrees, the incident angle of the one reflection before the final (N – 1 times reflections) has to be 'θ', which is angle of the two mirror wedge. N – 2 times reflection incident angle has to be '2θ' (see fig. 7). Briefly, the incident (first) angle α is proportional to the wedge angle θ and the number of reflection N. The equation of that relation is

$$\alpha = (N - 1)\,\theta \tag{16}$$

where 'α' is smaller than 90 degrees, N is greater than one and 'θ' is larger than zero degrees.

3.3 Sensitivity of the multiple reflection interferometer

The sensitivity of the multiple reflection interferometer when compared to the Michelson interferometer is related to the number of reflections. The following section of this thesis shows the displacement sensitivity of a multiple reflection interferometer.

3.3.1 Displacement sensitivity

The sensitivity of the standard Michelson interferometer is

$$\mathrm{D} = \frac{\lambda}{2} \tag{17}$$

and the displacement sensitivity is

$$D_s = \frac{\lambda}{4} \quad \text{(From equation 15)} \tag{18}$$

In the multiple reflection interferometer, the displacement sensitivity is

$$D_m = \frac{\lambda}{4} \cdot \frac{\sin\theta}{\sin N\theta} \tag{19}$$

where N is the total number of reflections, λ is the wavelength of the laser in the system and θ is the angle of the two-mirror wedge.

Fig. 8 shows the beam path details of the multiple reflection interferometer within the two-mirror wedge. Two mirrors, M1 and M2, meet at the point A, and θ is the angle of the two mirrors. The total path from b1 to b4 which satisfies an angle condition α = (N – 1) θ is exactly equal to the imaginary path from b1 to b'4.

$$\overline{b1\,b4} = \overline{b1\,b'4} \tag{20}$$

Figure 8 The motion of beam at the two-mirror wedge when the mirror is displaced by a distance ‘d’. [3]

A normal displacement d of mirror M2 to mirror M2' causes the optical path change from b'4 to b''4. The distance of the beam path is from b1 to b''4 when the mirror M2 moves to M2'. The displacement senstivity of the multiple reflection interferometer is

$$D_m = \overline{b1\, b''4} - \overline{b1\, b'4} = \overline{b'4\ \ b''4} = d' \tag{21}$$

$$d' = \overline{AA'} \cdot \sin N\theta \tag{22}$$

Also, distance A to A' can be expressed to

$$\overline{AA'} = \frac{d}{\sin\theta} \tag{23}$$

The eqaution (22) and (23) are

$$d' = \frac{d}{\sin\theta} \cdot \sin N\theta \tag{24}$$

To find the displacement sensitivity $D_{m,}$ starting in the mulitple reflection interferometer, the 'd' is replaced to 'd'' such that

$$\frac{\lambda}{2} = 2\ d' \tag{25}$$

where 'd'is the optical path difference. Then the result of two equation (24) and (25) can be written as

$$\frac{\lambda}{2} = 2\ \frac{d}{\sin\theta} \cdot \sin N\theta \tag{26}$$

The displacement sensitivity of the multiple reflection interferometer D_m is

$$D_m = d = \frac{\lambda}{4} \cdot \frac{\sin\theta}{\sin N\theta} \tag{27}$$

3.3.2 Effect of incident angle

Fig. 9 shows two different initial incident beam angles; (a) beam travels between two mirrors with small incident beam angle, (b) beam travels with a large angle. For example, in the case of fig. 9 (a), the beam travel change is almost 8·d, but case (b) shows that the optical travel path is longer than 8·d ('d' is displacement of mirror).

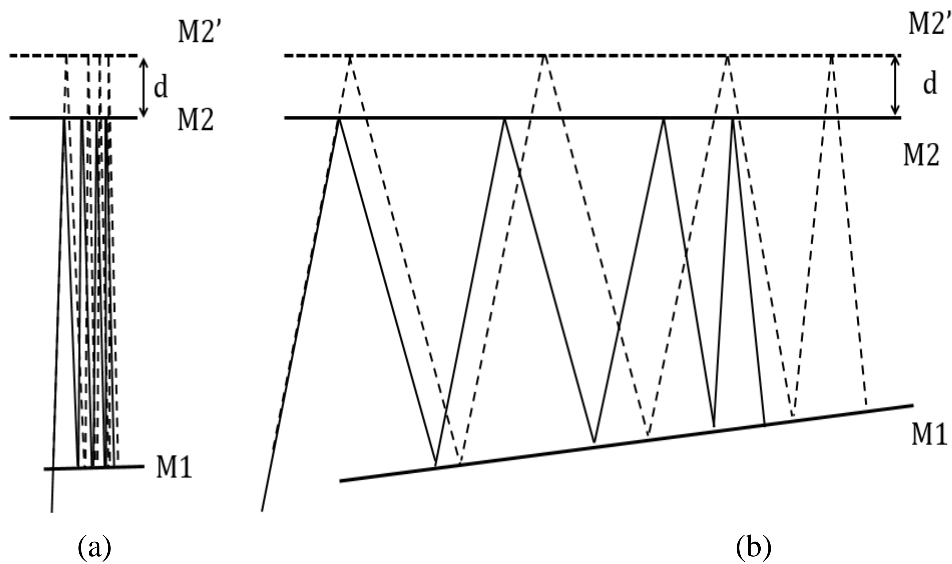

Figure 9 Optical path change when incidence angle is (a) small and (b) large between two mirrors. The solid line shows original beam moving path and dash-line shows a beam moving path after displacement of the mirror M2 [5]

This result is very important because it demonstrates that when the initial incident angle is very small, equation (27) can be expressed as

$$\frac{\sin(\theta)}{\sin(N\theta)} = \frac{1}{N}\ (when\ \theta < 1\ degree) \tag{28}$$

Thus, equation (27) can be changed to

$$\mathrm{d} = \frac{\lambda}{4N} \tag{29}$$

3.4 <u>Concept design for dual arm multi-reflection interferometer</u>

This dual arm multi-reflection interferometer is designed to realize identical angles between two tilted pairs of mirrors in both the arms by connecting them with a two gears assembly and rotation stages. Fig. 10 shows a general schematic diagram of this set up. In this arrangement, mirror 2 and mirror 4 are mounted at the center of the gear assembly and is at the center of the two rotation stages. Mirror 2 faces mirror 1 forming a wedged angle and the mirror 4 faces mirror 3 forming a wedged angle in the opposite direction. Furthermore, gear 1and gear 2 are meshed with their center fixed on two rotational stages. As a result, mirror 2 and 4 are able to rotate at the same time and by the same angle but in the opposite direction.

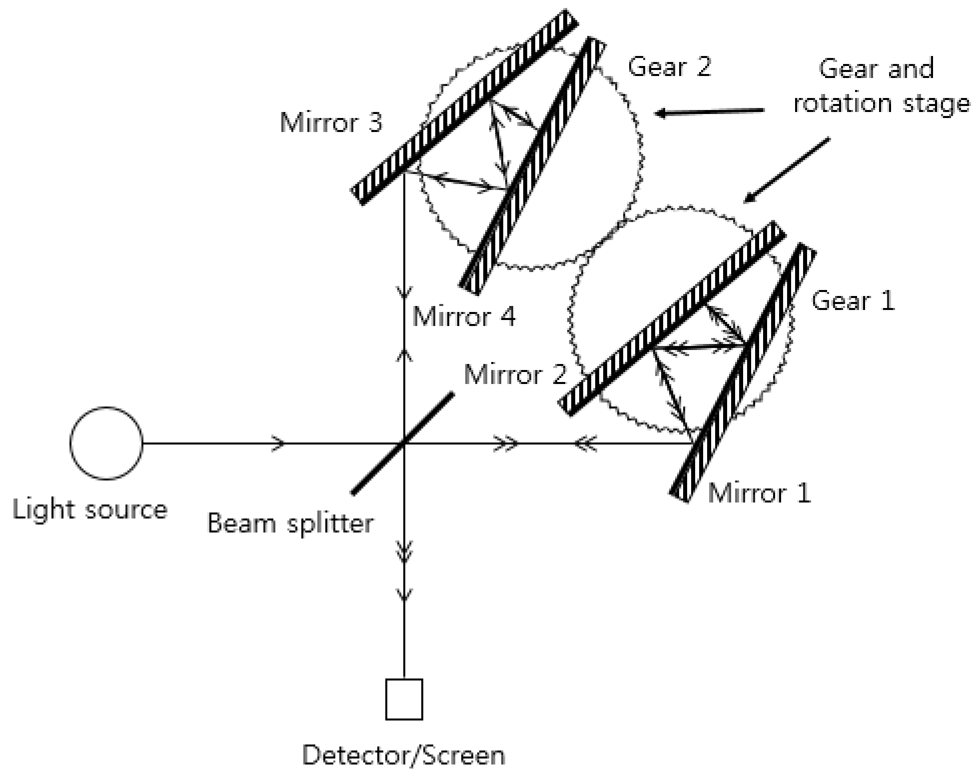

Figure 10 Schematic diagram of Dual Reflection Interferometer

If either mirror 2 or 4 is rotated, the wedge angle is the same in both the assemblies. In our system, mirror 2 is mounted on a PZT stage for introducing displacement. Once the system is set and aligned, the two arm multiple reflection interferometer will have the identical number of reflections in both the arms.

4. EXPERIMENT

The use of multiple reflections in a Michelson's arrangement has already been reported as mentioned in the previous chapter. The theoretical analysis shows that it is possible to obtain multiple reflections in the order of 1000 or more. If we assume that the average distance between the two mirrors is a few millimeters, we can expect the path difference between the multiple reflection arm and the single reflection arm of the interferometer to be greater than one meter. To reduce the optical path difference, the arm with the single reflection must be made larger. Thus, it is not possible to create a compact multiple reflection interferometer suitable for industrial applications. To solve this problem, we propose an alternate design where it is possible to generate the same number of reflections in both the arms of the interferometer. It is normally possible to create an arbitrary number of multiple of reflections in both the arms by having a separate and independent mirror arrangement. However, this arrangement becomes much harder to manage and align if the number of reflection becomes larger. In order to make alignment easier and compact, the design in this proposal is to connect both the mirrors in one assembly by a system of gears to maintain the same number of reflections in both the arms.

One such proposed assembly is shown in fig. 11. Two rotational stages are placed side by side with the center of rotation separated by a difference of '2a' between them.

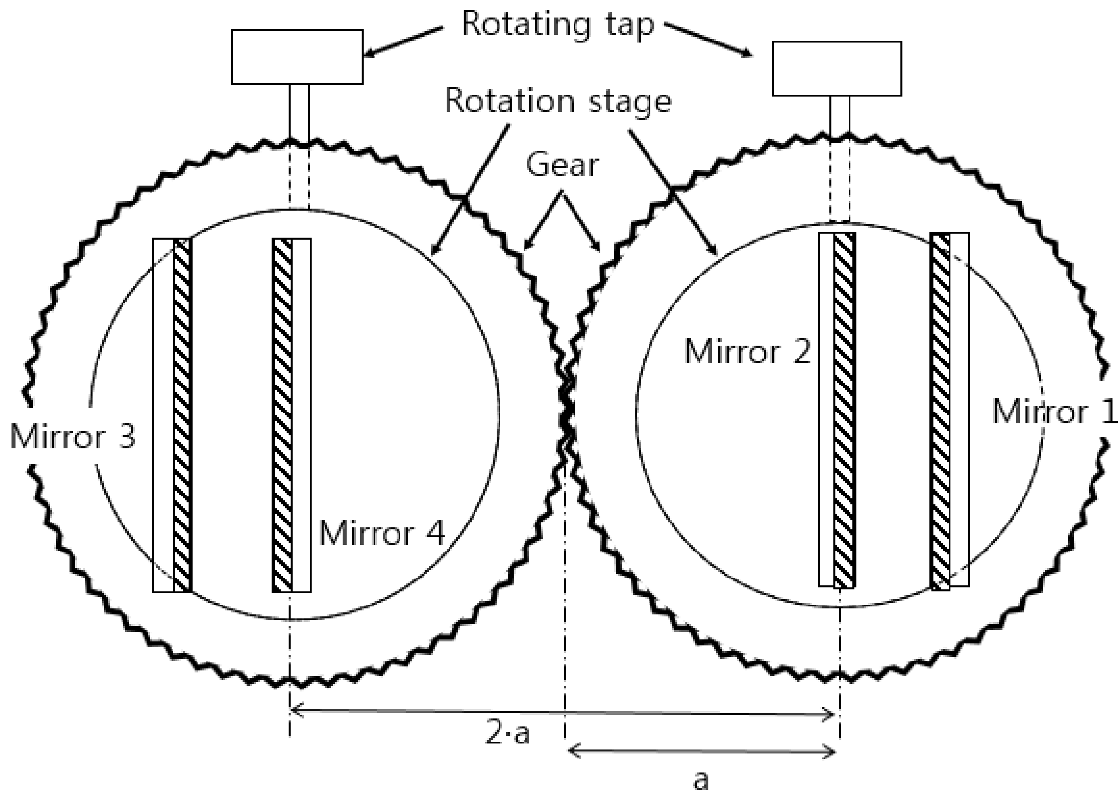

Figure 11 Location of gears, mirrors, and rotational stage in schematic view; Mirror 3 and 1 are fixed mirrors and these mirrors are connected by a magnet based stage. Mirror 2 and 4 are mounted on gears. The gears are meshed at a distance 'a' (a is 3 inches). The rotating tab is able to rotate the stage in 0.04 degree increments.

Two large circular gears of radius 'a' are mounted at the center of the rotational stage so that the two mesh. Two mirrors are mounted at the center of rotation of the two stages as

shown in the fig. 11. When one of the stages is rotated, the two mirrors move in the opposite direction, thus creating the same angle of tilt in mirror 2 and mirror 4. The minimum angle of rotation that can be measured with this rotation stage is 0.04 degrees. However, smaller rotational angles are possible but not measurable.

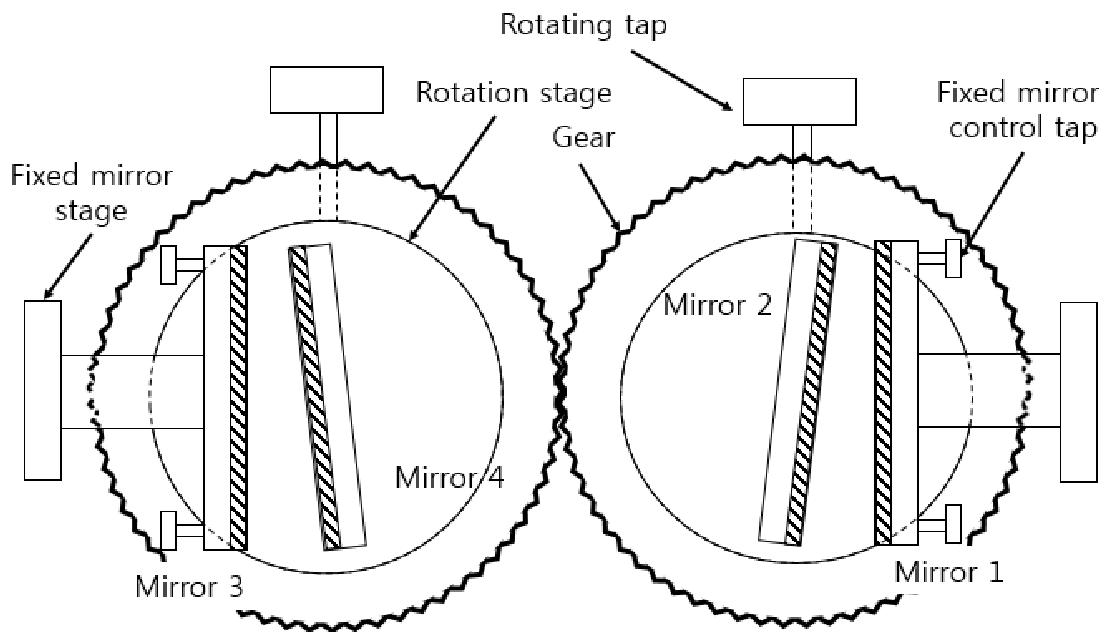

Figure 12 Schematic diagram of 4 mirrors in the dual arm multiple reflection interferometer after rotating the gear.

Fig. 12 shows with schematic diagram of the location of the fixed mirrors after rotation. When one of the rotational stages is moved by an angle of ‘α’, the mirrors are both

rotated by the same magnitude of ‘α’ but in the opposite directions. This set of measurements maintains the same angle between the mirror 1 and 2 and mirror 3 and 4. The schematic of the experimental arrangement of the modified Michelson’s interferometer setup with the beam splitter and entire reflection paths are shown in fig. 13.

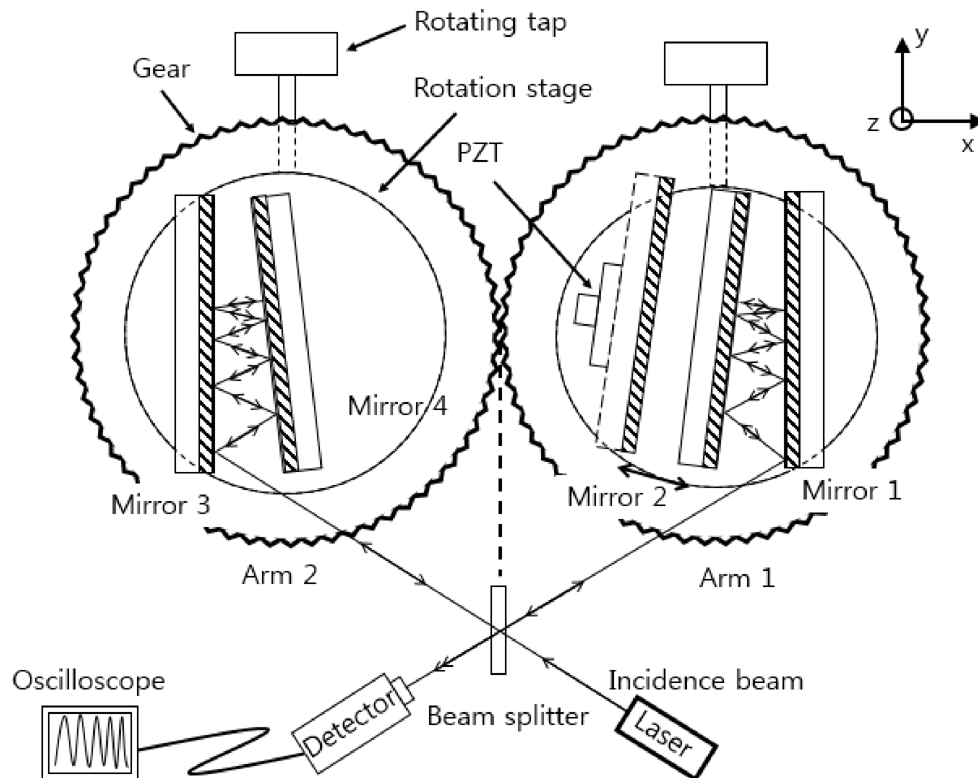

Figure 13 Modified multiple reflection Michelson interferometer

A He-Ne laser beam is incident such that it is at an arbitrary angle entering the setup. The beam splitter is located at the center where the two gears mesh. The reflected beam from the beam splitter forms arm 2 of the interferometer and the transmitted beam forms arm 1. The beams go through multiple reflections in both the arms and the beam retraces its path back to the beam splitter and combine at the beam splitter. To be able to make quantitative measurements on the number of reflections, mirror 1 is mounted on a PZT stage that can be displaced along the x-y plane. The phase difference introduced by the PZT mirror movement is amplified by the number of reflections.

4.1 Experimental set-up

In the experiment, the light source is a helium-neon (He-Ne) laser**.** The laser beam is divergent in both the arms of the interferometer and therefore it does not affect the final fringe formation. However, a collimated beam is recommended for a large number of beam reflections because the beam diameter gets larger in the case of multiple reflection. A 50/50 beam splitter is used to split the beam into equal amplitudes. A total of four mirrors are used, mirror 1 and 3 are fixed, mirror 2 and 4 are mounted on a 3 inch diameter gear. These two mirrors are connected as shown in fig. 14. The gears are mounted on two rotational stages, which are able to rotate 360 degrees with a minimum measurable angle of rotation being 0.04 degrees. The error in the angle of measurement is 0.004 degrees

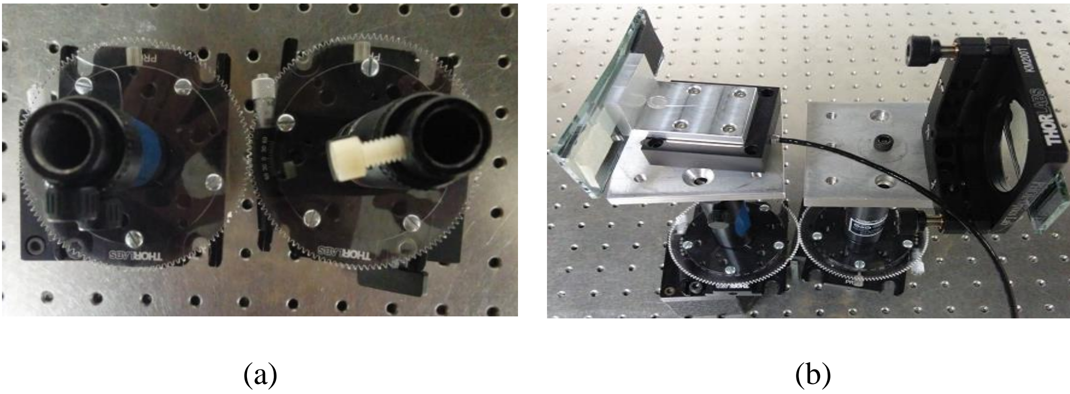

(a) (b)

Figure 14 (a) Two 3 inch gears on the magnet base and (b) PZT mirror and normal mirror set on the gears.

Each mirror is mounted on a separate stage which can be tilted about the x and y axis.

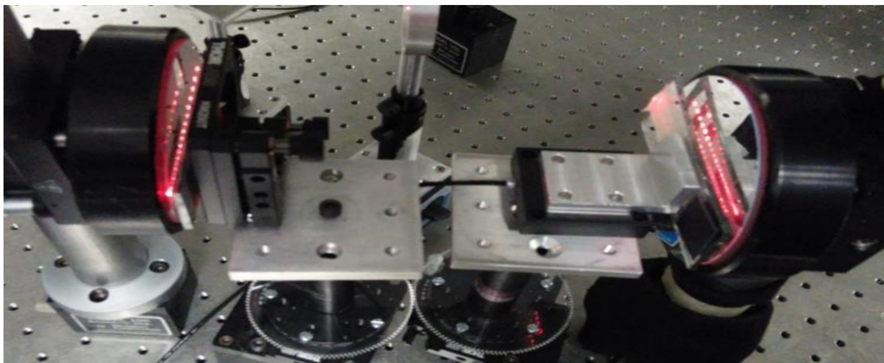

Figure 15 Picture of the beam reflection through the wedge shape mirror arms. Outside mirrors were fixed and inside mirrors were mounted on the 3 inch gear and rotation stage.

Fig. 15 shows the photograph of the dual multiple reflection assembly. Two separate mirror systems with an angle between them are located at the same distance from the contact position of the gear. The number of beam reflections in each arm can be increased or decreased simultaneously. One of the mirrors is mounted on a PZT stage which can be displacement by a high voltage power supply. A ramp signal is input to the high voltage supply and this causes the mirror to move back and forth. The mirror movement causes the interference pattern to fluctuate between bright and dark spots on a laser power meter head.

4.2 Experimental procedures

Two different experiments are conducted to test this dual arm multiple reflection interferometer. The first experiment is to determine the importance of the incidence angle on the number of beam reflections. The second experiment is to measure the displacement sensitivity of the dual arm multi-reflection interferometer based on the numerical increment of beam reflection numbers, and comparing it to theoretical value of the displacement for a given incident angle.

4.2.1 Displacement sensitivity difference by incidence angle

The first experiment investigated the relation of the incidence angle of the beam and the displacement sensitivity, which is expressed by the equation (29). Equations (27)

and (29) show the relationship of the displacement sensitivity, and fig. 9 shows that if the incidence angle is large, the beam will not be able to retrace its path and will eventually exit the mirror assembly on the opposite side. The first investigation is used to identify some of the conditions of the angle of incident for the interferometer. Initially, the two pair of mirrors are aligned parallel to each other. Then the rotational stage is used to rotate mirrors such that the reflected beams inside the dual pairs of mirror assembly retraces its path. Mirror 1 and 3 are rotated by 20°, 15°, 10°, 5°, and 1° of wedge angles. Mirror 2 is mounted on PZT device, driven by a program (PIMikroMove ™). Finally, the displacement sensitivity is measured. The results of 1 and 20 degree are compared in section 5.2.

A software is developed in MATLAB (APPENDIX A) which can calculate the number of reflections according to wedge shape mirror angle and beam incident angle. This program is used if the incidence angle, two mirror angle, and reflection numbers do not followed the equation (19) [17] because the geometry is other than a wedge shape such as curve or roof top mirror shape. This program allows the reflection number to be calculated and simulated. It draws the mirror assembly first, which includes the inclined top line and the straight bottom line in fig. 16, and then it traces the beam; the mirror assembly and beam movement are defined by the user. If the mirror assembly and beam data are set, a solid line is drawn which shows the beam undergoing multiple reflections in the mirror assembly. When the beam hits the top or the bottom line, it is reflected by

the incident angle. Fig. 16 shows the program interface with input data boxes and a simulation of the beam movement.

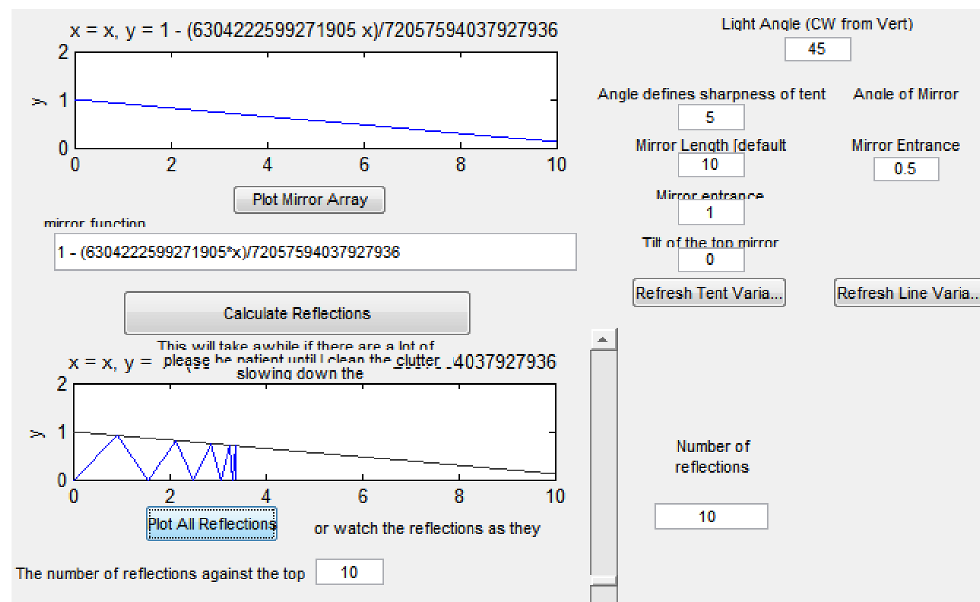

Figure 16 A reflection number calculating program according to mirror and incident angel. The wedge shape angle and beam incident angle are 45 degree

In the right upper side of fig. 16 the actual values of the mirror angles and beam incident angle are entered. The top left side graph in fig. 16 shows the shape and angle of the two mirror set which is programed as straight lines. The inclined line depicts the top mirror and the bottom line is the second mirrors. The second graph shows the simulation

of beam motion with the two mirrors. This shows the beam reflection with a 5 degree wedge angle and a 45 degree incidence angle for a total of 10 reflections.

4.2.2 Displacement sensitivity with multiple reflection

The experiment was to measure the displacement sensitivity of the dual arm multi-reflection interferometer. The displacement sensitivity is measured as the number of reflections is increased gradually by rotating the gear assembly. At specific angles, the reflected beam will be observed to combine at the beam splitter. By adjusting the tilt about the y and x axis, the beams can be aligned such that they are collinear. The beams are adjusted such that only one interference maximum or minimum occurs. The next higher reflection order can be generated by gradually increasing the angle between the mirrors by rotating the gear assembly. In this experiment the incidence angle is set close to 0.5 degree by tilting mirror 1 and 3 and the number of reflections are gradually increased. Mirror 2 and 4 are also rotated similarly in order to increase by the same number of reflections. Mirror 2 is mounted on a PZT device and moves 500, 1000, and 2000 nm. The reason for displacing the mirror by different distances is to test the validity of the displacement sensitivity measurement. For a given wedge and incident angles, the sensitivity should be consistent regardless of the PZT mirrors displacement. The detector detects an interference signal caused by the two beams from both the arms of the interferometer and the oscilloscope displays the fluctuating signal. The oscillating voltage

from the oscilloscope can be converted to excel files. From the excel data the total number of cycles can be determined. This number is then divided by the total mirror’s movement.

5. RESULT

The sensitivity of the dual arm multi-reflection interferometer is evaluated by observing the total phase cycle the interferometer goes through for a given mirror displacement. From analyzing the signal the experimental value of the number of multiple reflections is determined.

5.1 Relationship between incidence angle and wedge shape mirror angle

Fig. 17 shows the plot of the number of beam reflections inside the wedge angle calculated by equation (16). A higher reflection number requires a smaller angle between the two mirrors. For example, if the angle of incidence and wedge mirror are set to 5 degree and 0.5 degree respectively, the reflection number is 11. In another situation, if the wedged shape mirror is set at 0.1 degrees and the incidence angle is 10 degrees, the reflection number is 101.

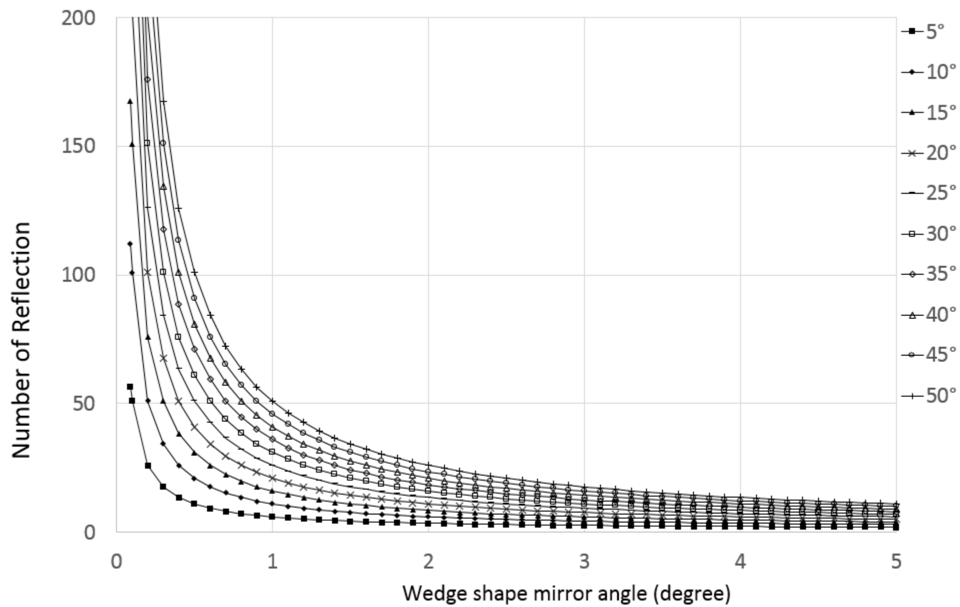

Figure 17 Diagram of the beam reflection number with different incident angle and wedge shape mirror angle

Theoretically, the number of beam reflections can be 1000 or more if it satisfies specific conditions. For example, if the incident angle is 50 degrees and the wedge angle is 0.05 degrees the number of reflections is 1000. However, the higher incidence angle restricts the mirror length and also requires that the distance between two mirrors be as small as possible. As the initial angle is increased, the beam path on the x-axis direction is expanded as shown in fig 9. This means that the larger initial angle needs a longer mirror even though the number of reflections is low.

5.2 Displacement sensitivity difference by incidence angle

The first experiment demonstrates the relationship between incidence beam angle and optical path length difference. Fig. 18 and Fig. 19 show the profile of the signals from the detector and observed in the oscilloscope measured under the same conditions but with different incidence angles. The total number of reflections is two, and the piezo mirror moves in increments of 475 nm. The incident beam angle for fig. 18 is less than 1 degree and for fig. 19 it is 20 degrees. This angle difference results in different optical path lengths and sensitivities. For a mirror translation of 475 nm backward and forward using a ramp signal, the fringe pattern cycle of 1 degree experiment is 6.330 nm and 20 degree experiment is 7.006 nm. This means that a 75.039 nm mirror displacement is needed to change from a bright fringe to a dark fringe for 1 degree incident angle as shown fig. 18. A 67.799 nm movement is needed for one cycle for 20 degrees incident angle as shown fig. 19. These results show that equation (28) can not apply to all multiple reflection interferometers. When the initial angle is larger than one degree, it follows equation (27).

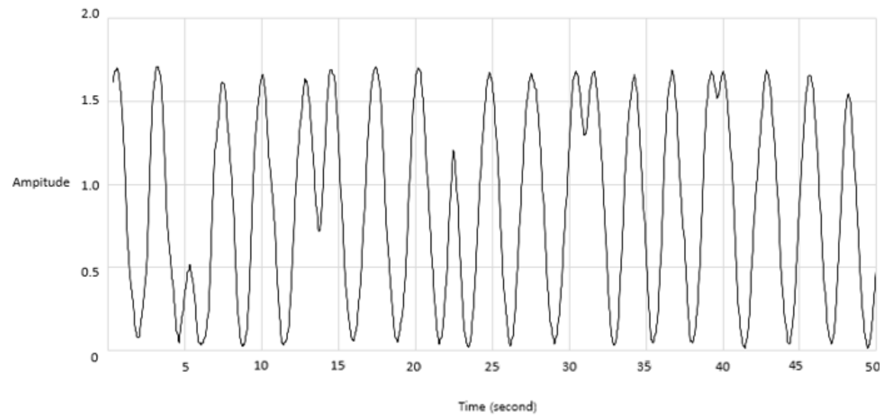

Figure 18 The detector signal for the fringe pattern changed when the incidence angle and wedge-mirror angle are one degree. The x-axis is the time during the mirror displacement and y-axis is the signal from the photo detector.

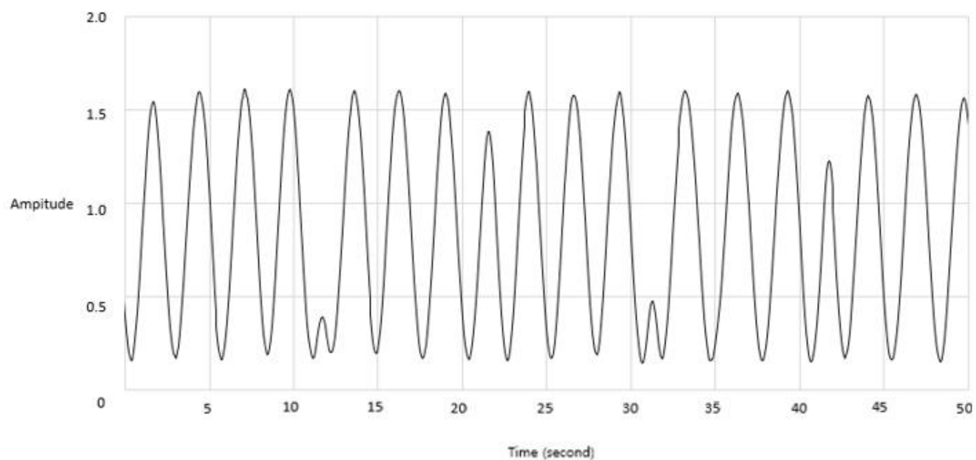

Figure 19 The detector signal for the fringe pattern changed when the incidence angle and wedge-mirror angle are 20 degrees.

5.3 Displacement sensitivity of multiple reflection

The second experiment is that the sensitivity is incrementally change in the Michelson interferometer through multiple reflection by changing the wedge angle and incident angle. It can be observed that as the number of reflection increases for a fixed PZT displacement the number of cycles increases appropriately. The figures below show the number of oscillations as a function of constant PZT mirror displacement and beam reflection number.

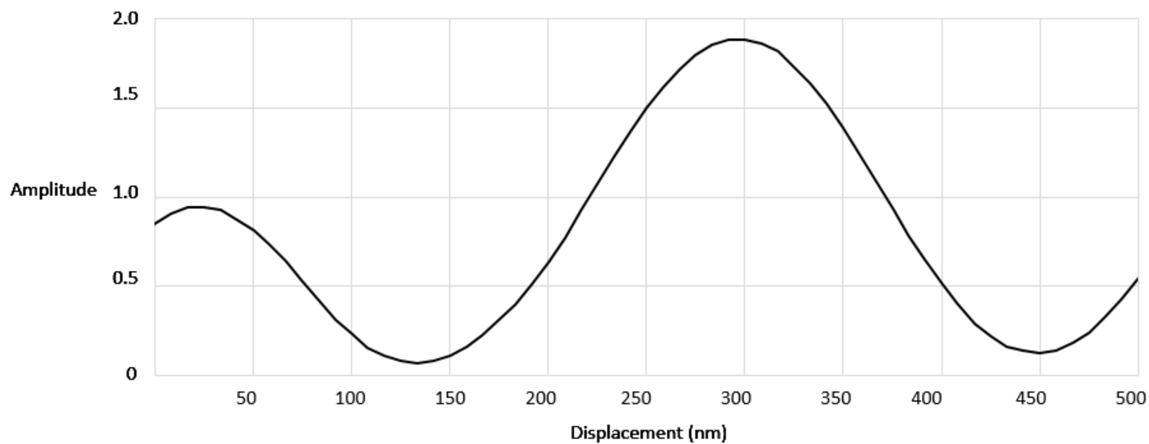

Figure 20 Typical Michelson interferometer (1 reflection)

Fig. 20 shows a result of the typical Michelson interferometer. The graph shows the optical power change depending on the mirror displacement. Approximately 157.6

nm mirror movement results an amplitude change from min to max. The next figure shows a result for two reflections.

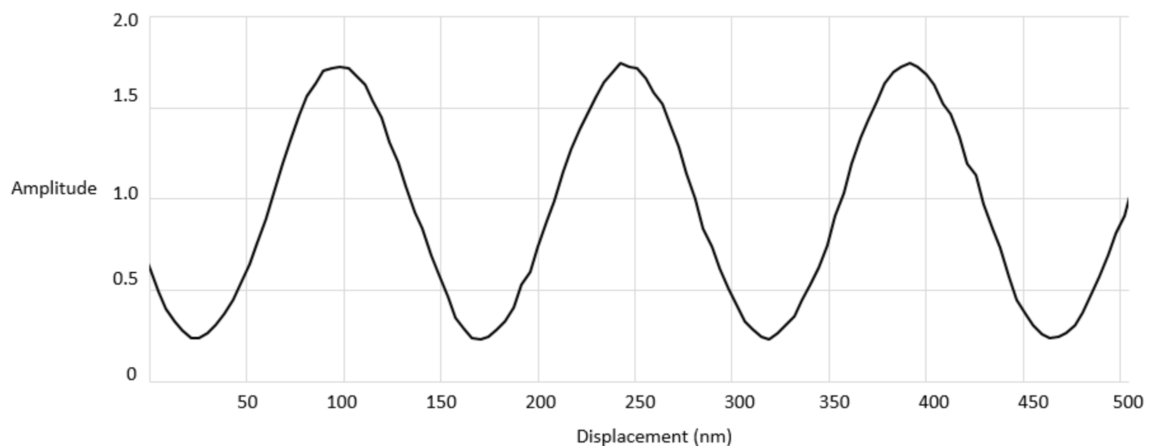

Figure 21 Multiple reflection interferometer (2 reflections)

Fig. 21 shows a detector signal tracing for a mirror movement of 500 nm in a two reflection interferometer. Theoretically, a two reflection system has twice the sensitivity of a one reflection interferometer. The graph illustrates that the amplitude fluctuation number is 3.909 between 100 nm and 400 nm mirror translation and its value shows a 76.740 nm displacement sensitivity. The result has twice the displacement sensitivity than in one reflection interferometer displacement sensitivity. This experiment are carried out for 12, 25, 50,70 and 110 reflections..

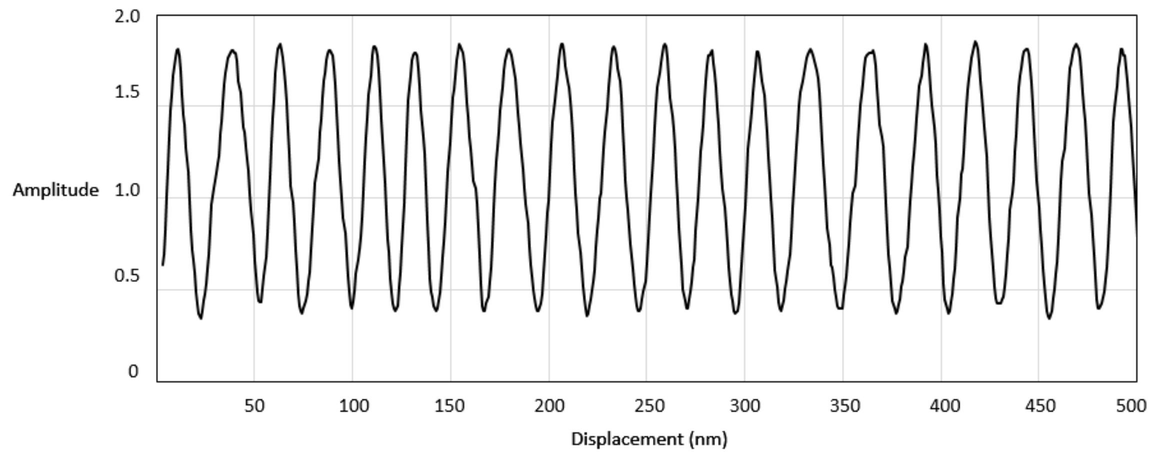

Figure 22 Multiple reflection interferometer (12 reflections)

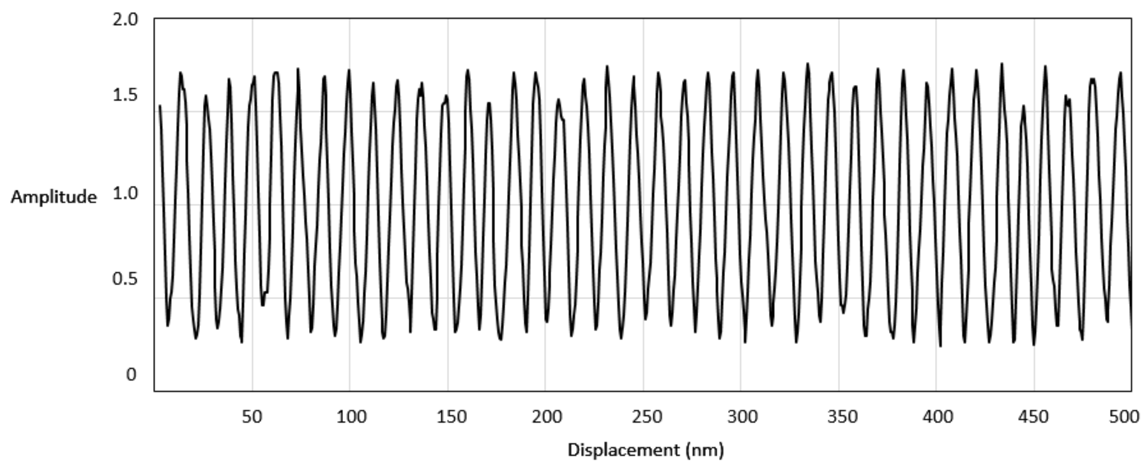

Figure 23 Multiple reflection interferometer (25 reflections)

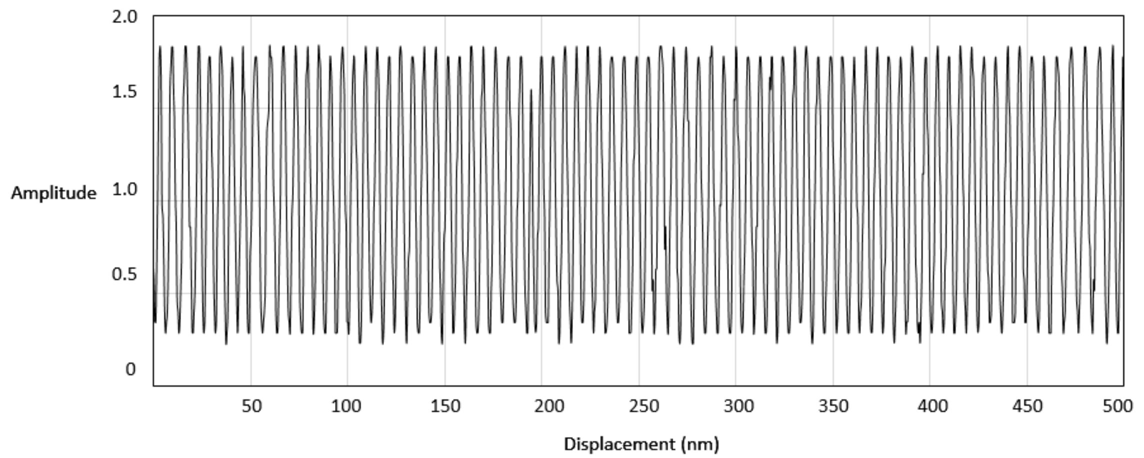

Figure 24 Multiple reflection interferometer (50 reflections)

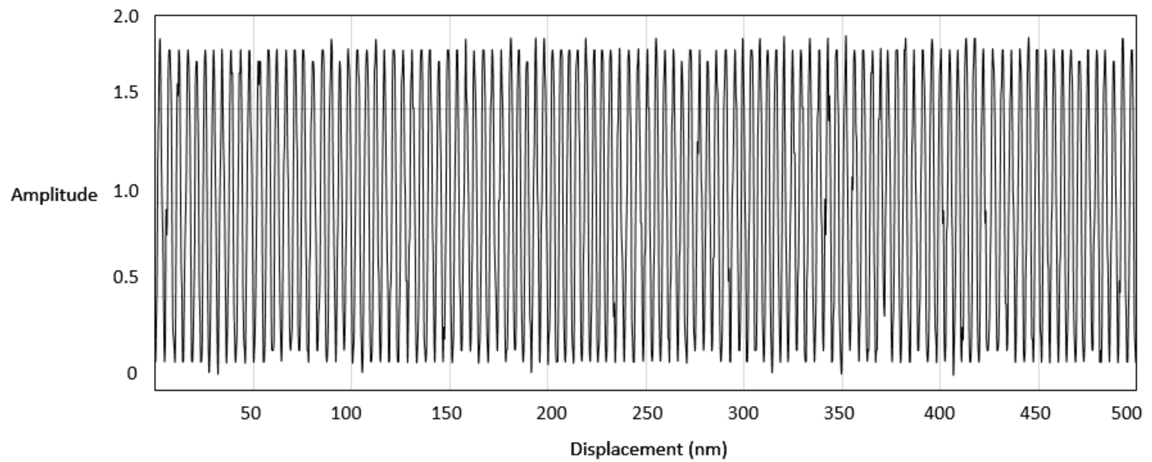

Figure 25 Multiple reflection interferometer (70 reflections)

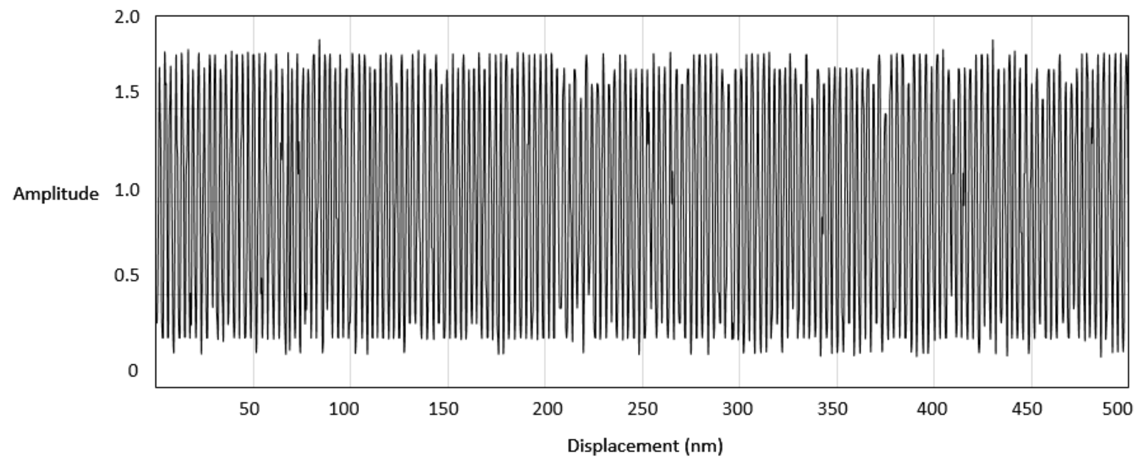

Figure 26 Multiple reflection interferometer (110 reflections)

It can be seen that 12, 25, 50, 70, and 110 reflections have 12.782, 6.461, 3.209, 2.228, and 1.451 nm displacement sensitivity respectively. Table 1 shows the displacement sensitivity based on the PZT mirror movement as the range of the PZT displacement is increased. The result shows the displacement sensitivity moves at an arithmetic progression as the number of reflections increase.

Table 1 Displacement sensitivity according to PZT mirror displacement of 500, 1000 and 2000 nm and its average result

Reflection Number	Displacement Sensitivity (nm) according to mirror movement			Average (nm)	Standard Deviation
	500 nm	1000 nm	2000 nm		
1	157.604	157.540	159.464	158.203	0.892
2	76.740	77.971	78.734	77.815	0.821
3	51.888	52.423	52.166	52.159	0.218
4	38.889	39.596	39.188	39.224	0.290
5	31.223	31.797	31.267	31.429	0.261
6	25.290	27.197	26.168	26.218	0.779
7	22.693	22.341	22.433	22.489	0.149
10	16.282	15.202	15.810	15.765	0.442
12	12.782	13.515	13.136	13.144	0.299
15	10.750	10.342	10.471	10.521	0.170
20	8.113	7.665	7.908	7.895	0.183
25	6.461	6.169	6.325	6.318	0.119
30	5.386	5.153	5.260	5.266	0.095

50	3.209	3.134	3.142	3.161	0.034
70	2.228	2.298	2.251	2.259	0.029
100	1.561	1.595	1.588	1.581	0.014
110	1.451	1.427	1.435	1.438	0.010

Fig. 27 shows the graph of the average displacement sensitivity and fig. 28 and table 2 shows the errors between the values calculated from the equation and experimental results. The theoretical equation used for analysis is equation (27).

Table 2 Displacement sensitivity of a multiple reflection interferometer and its error when compared with theory.

Reflection Number	Displacement Sensitivity (nm)		Error (nm)
	Theoretical	Experimental	
1	158.200	158.203	0.003254
2	79.100	77.815	1.285013
3	52.733	52.159	0.574240
4	39.550	39.224	0.325764
5	31.640	31.429	0.210733
6	26.367	26.218	0.148375

7	22.600	22.489	0.110832
10	15.820	15.765	0.055391
12	13.183	13.144	0.039190
15	10.547	10.521	0.025646
20	7.910	7.895	0.014748
25	6.328	6.318	0.009645
30	5.273	5.2665	0.006841
50	3.164	3.161	0.002515
70	2.260	2.259	0.001310
100	1.582	1.581	0.000655
110	1.438	1.438	0.000551

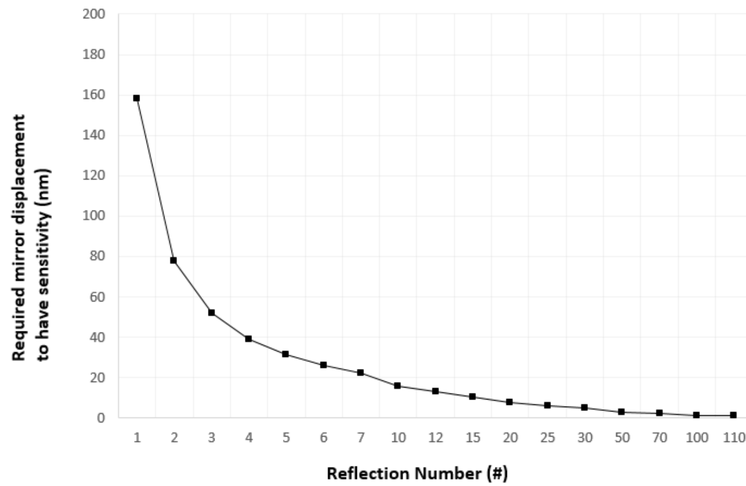

Figure 27 Average Displacement Sensitivity of 632.8 nm He-Ne laser according to reflection number

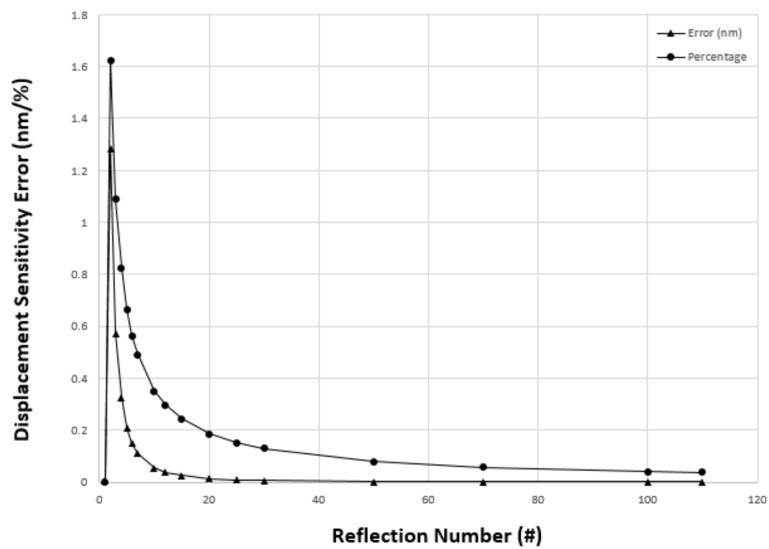

Figure 28 Displacement sensitivity error depending on reflection number in distance (nm) and percentage

Table 2 shows the equation (27) displacement sensitivity, the experimental sensitivity and the error of those two results according to the number of reflections in the wedge shape mirror. It is shown that the sensitivity decreases dramatically for the first seven reflections then the rate of decrease is much reduced after 50 reflections. After 100 reflections, it starts to converge slowly. The error is computed as the difference of the theoretical and experimental values and it is stated as a percentage of the theoretical value. The highest error value percentage is 1.62 % when the number of reflections is two. The error continues to become smaller as the reflection number increases.

In this experiment, the displacement sensitivity of 1.438 nm is achieved at 110 reflections. Error exists only in the pico meter range. As shown in the table 1, the sensitivity has been determined for different displacement of the PZT and the sensitivity was found to be consistent for a given number of reflections regardless of the PZT mirror movement.

6. CONCLUSION

Michelson interferometer has been researched and applied in many different fields and developed. The dual arm multiple reflection interferometer can be used to increase the sensitivity of measurements. However, having a separate mirror assembly has a limitation, for example, it is not convenient to control the number of reflections in both the arms to make them the same. Once the dual arm multiple interferometer is set up for a specific sensitivity, the whole mirror assembly must be realigned to convert it to a different sensitivity of system. A one arm reflection structure proposed in this thesis with a combined gear assembly requires modification of the other arm position or angle but the two arm reflection system requires only one rotation which automatically matches the optical path length between the two arms. Once this new system is stabilized, the concern is extraneous noise and erratic displacement of the mirror. Also beam absorption is another issue because the beam is reflected multiple times in the mirror assembly. This system used a total of four mirrors and each reflection cases a reduction in the laser power because of absorption. This mirror absorption problem in not a big issue in small number of reflections but for a large number of reflections the reflected light will be reduced considerably due to absorption at each reflection.

7. FUTURE WORK

This dual arm multi-reflection is an improvement from the single arm multiple reflection Michelson interferometer. A different versions of the wedge-mirror shape such as roof top or curved shape mirror can be used to increase the number of beam reflections. Fig. 29 is an example which has not been implemented.

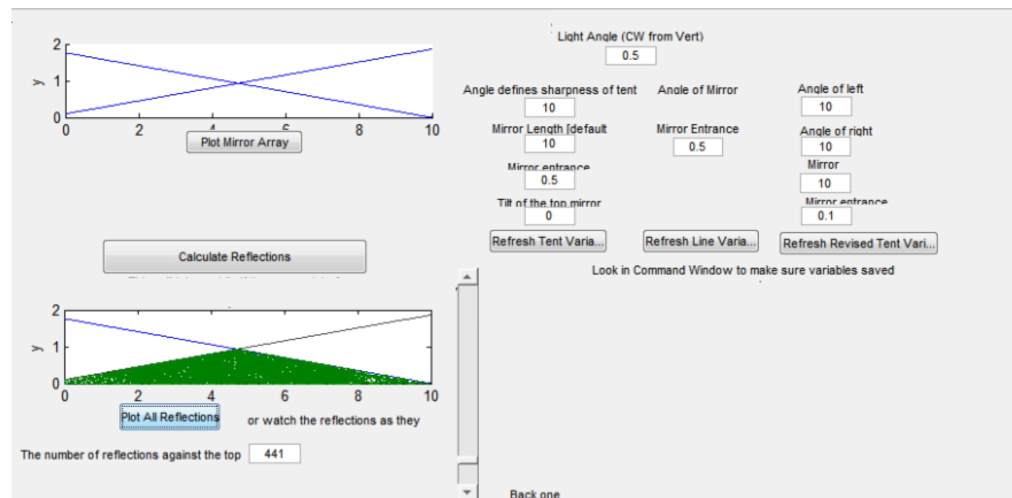

Figure 29 The simulation of beam reflection in the roof top mirror design with the same scale of the wedge shape

The number of beam reflections can be increased with the same incident angle. Also, the noise from external vibrations can be reduced using Fourier transform technique.

LIST OF REFERENCES

[1] Albert A. Michelson and Edward W. Morley, “On the Relative Motion of the Earth and the Luminiferous Ether”, AM. Jour. Sci. **34** (1887): 330-345.

[2] R. S. Shankland, "Michelson–Morley experiment". Am. J. Phys, **32** (1964): 16.

[3] S. Chandra and R. S. Rohde, "Ultrasensitive multiple-reflections interferometer". APPLIED OPTICS, **21** (1982): 9.

[4] Doo Hee Lee, and Byoung Yoon Kim, “Multiple-reflection interferometer for high accuracy measurement of small vibration displacement”, Rev. of Sci. Inttr, 71 (2000).

[5] Marco Pisani, “Multiple reflection Michelson interferometer with picometer resolution”, OPTICS EXPRESS, **16** (2008): 26.

[6] N. Krstajic, D. Childs, R. Smallwood, R. Hogg and S. J. Matcher, “Common path Michelson interferometer based on multiple reflections within the sample arm: sensor applications and imaging artefacts”, IOP. Meas. Sci. Technol, **22** (2011): 207002.

[7] C. M. Sutton, “Non-linearity in length measurement using heterodyne laser Michelson interferometry”, IOP. J. Phys. E: Sci. Instrum, **20** (1987): 1290-1292.

[8] M. Tanaka and K. Nakayama, “A New Optical Interferometer for Absolute Measurement of Linear Displacement in the Subnometer Range”, IOP. Japanese Journal of Applied Physics, **22** (1983): L233-L235.

[9] M. Pisani and M. Astrua, “Angle amplification for nanoradian measurements”, APPLIED OPTICS, **45** (2006): 1725-1729.

[10] M. Pisani, “A homodyne Michelson interferometer with sub-picometer resolution”, IOP. Meas. Sci. Technol. **20** (2009): 084008.

[11] N. Yim, C. Eom and S. Kim, “Dual mode phase measurement for optical heterodyne interferometry”, IOP. Meas. Sci. Technol. **11** (2000): 1131-1137.

[12] D. Su, M. Chiu and C. Chen, “Simple two-frequency laser”, Precision Engineering, **18** (1996): 161-163.

[13] K. Chen, H. Chin, J. Chen and T. Chen, “An alternative method for measuring small displacements with differential phase difference of dual-prism and heterodyne interferometry”, ELSEVIER. Measurement, **45** (2012): 1510-1514.

[14] V. E. Gherm, N. N. Zernov and B. Lundborg, “The two-frequency, two-time coherence function for the fluctuating ionosphere: wideband pulse propagation”, Journal of Atmospheric and Solar-Terrestrial Physics, 59 (1997): 1843-1854.

[15] V. E. Gherm, N. N. Zernov, B. Lundborg and A. Vastberg, “The two-frequency coherence function for the fluctuationg ionosphere: narrowband pulse propagation”, Journal of Atmospheric and Solar-Terrestrial Physics, 59 (1997): 1831-1841.

[16] Eugene, Hecht. OPTICS 4th. San Francisco: Addison Wesley, 2002.

[17] C. Joenathan, A. Bernal and C. Hakoda, “Modified and improved multiple reflection interferometer for high sensitivity measurements”, Private communication, Project report, Rose-Hulman Institute of Technology, (2013)

APPENDIX A

Appendix A shows a MATLAB program code of the beam reflection calculation and simulation developed by Chirstopher Hakoda.

```
function varargout = MultipleReflectionsGUI(varargin)
gui_Singleton = 1;
gui_State = struct('gui_Name',       mfilename, ...
                   'gui_Singleton',  gui_Singleton, ...
                   'gui_OpeningFcn', @MultipleReflectionsGUI_OpeningFcn, ...
                   'gui_OutputFcn',  @MultipleReflectionsGUI_OutputFcn, ...
                   'gui_LayoutFcn',  [] , ...
                   'gui_Callback',   []);
if nargin && ischar(varargin{1})
    gui_State.gui_Callback = str2func(varargin{1});
end
if nargout
    [varargout{1:nargout}] = gui_mainfcn(gui_State, varargin{:});
else
```

```
    gui_mainfcn(gui_State, varargin{:});
end
function MultipleReflectionsGUI_OpeningFcn(hObject, eventdata, handles, varargin)
handles.output = hObject;
guidata(hObject, handles);
function varargout = MultipleReflectionsGUI_OutputFcn(hObject, eventdata, handles)
varargout{1} = handles.output;
function edit1_Callback(hObject, eventdata, handles)
lightAngle = get(hObject,'String');
lightAngle = str2num(lightAngle);
save lightAngle
function edit1_CreateFcn(hObject, eventdata, handles)
if ispc && isequal(get(hObject,'BackgroundColor'),
get(0,'defaultUicontrolBackgroundColor'))
    set(hObject,'BackgroundColor','white');
end
function edit2_Callback(hObject, eventdata, handles)
arcAngle = get(hObject,'String');
arcAngle = str2num(arcAngle);
save arcAngle
```

```
function edit2_CreateFcn(hObject, eventdata, handles)
if ispc && isequal(get(hObject,'BackgroundColor'),
get(0,'defaultUicontrolBackgroundColor'))
    set(hObject,'BackgroundColor','white');
end
function edit3_Callback(hObject, eventdata, handles)
mirrorLength = get(hObject,'String');
mirrorLength = str2num(mirrorLength);
save mirrorLength
function edit3_CreateFcn(hObject, eventdata, handles)
if ispc && isequal(get(hObject,'BackgroundColor'),
get(0,'defaultUicontrolBackgroundColor'))
    set(hObject,'BackgroundColor','white');
end
function edit4_Callback(hObject, eventdata, handles)
gapHeight = get(hObject,'String');
gapHeight = str2num(gapHeight);
save gapHeight
function edit4_CreateFcn(hObject, eventdata, handles)
```

```
if ispc && isequal(get(hObject,'BackgroundColor'),
get(0,'defaultUicontrolBackgroundColor'))
    set(hObject,'BackgroundColor','white');
end
function edit5_Callback(hObject, eventdata, handles)
mirrorTilt = get(hObject,'String');
mirrorTilt = str2num(mirrorTilt);
save mirrorTilt
function edit5_CreateFcn(hObject, eventdata, handles)
if ispc && isequal(get(hObject,'BackgroundColor'),
get(0,'defaultUicontrolBackgroundColor'))
    set(hObject,'BackgroundColor','white');
end
function pushbutton1_Callback(hObject, eventdata, handles)
axes(handles.axes1);
syms x
cla;
load('previewD')
ezplot(x,fx, [0 10 0 2]);
axis([0 10 0 2]);
```

```
set(handles.edit7, 'String', char(fx));
guidata(hObject,handles)
function pushbutton2_Callback(hObject, eventdata, handles)
tentMirror()
function edit7_Callback(hObject, eventdata, handles)
function edit7_CreateFcn(hObject, eventdata, handles)
if ispc && isequal(get(hObject,'BackgroundColor'),
get(0,'defaultUicontrolBackgroundColor'))
    set(hObject,'BackgroundColor','white');
end
function pushbutton3_Callback(hObject, eventdata, handles)
ComputeReflections()
function pushbutton4_Callback(hObject, eventdata, handles)
axes(handles.axes2);
syms x
cla;
load('previewD')
load('computeD','vecx','vecy','number')
ezplot(x,fx,[0 10 0 2]);
hold all
```

```
plot(vecx,vecy);
axis([0 10 0 2]);
set(handles.edit8, 'String', int2str(number));
function edit8_Callback(hObject, eventdata, handles)
function edit8_CreateFcn(hObject, eventdata, handles)
if ispc && isequal(get(hObject,'BackgroundColor'),
get(0,'defaultUicontrolBackgroundColor'))
    set(hObject,'BackgroundColor','white');
end
function slider1_Callback(hObject, eventdata, handles)
slider = get(hObject,'Value');
slider = (slider*100)+2;
axes(handles.axes2);
cla;
load('previewD')
load('computeD','vecx','vecy','number')
hold on
syms x
ezplot(x,fx, [0 10 0 2]);
for i=2:slider
```

```
plot([vecx(i-1),vecx(i)],[vecy(i-1),vecy(i)]);
set(handles.edit9, 'String', int2str(i));
if i >= (number+1)
    set(handles.edit8, 'String', int2str(number));
    break
end
end
axis([0 10 0 2]);
hold off
function slider1_CreateFcn(hObject, eventdata, handles)
if isequal(get(hObject,'BackgroundColor'), get(0,'defaultUicontrolBackgroundColor'))
    set(hObject,'BackgroundColor',[.9 .9 .9]);
end
function edit9_Callback(hObject, eventdata, handles)
function edit9_CreateFcn(hObject, eventdata, handles)
if ispc && isequal(get(hObject,'BackgroundColor'),
get(0,'defaultUicontrolBackgroundColor'))
    set(hObject,'BackgroundColor','white');
end
function edit11_Callback(hObject, eventdata, handles)
```

```
arcAngle = get(hObject,'String');
arcAngle = str2num(arcAngle);
save mirrorAngle
function edit11_CreateFcn(hObject, eventdata, handles)
if ispc && isequal(get(hObject,'BackgroundColor'),
get(0,'defaultUicontrolBackgroundColor'))
    set(hObject,'BackgroundColor','white');
end
function edit12_Callback(hObject, eventdata, handles)
gapHeight = get(hObject,'String');
gapHeight = str2num(gapHeight);
save gapHeight
function edit12_CreateFcn(hObject, eventdata, handles)
if ispc && isequal(get(hObject,'BackgroundColor'),
get(0,'defaultUicontrolBackgroundColor'))
    set(hObject,'BackgroundColor','white');
end
function pushbutton5_Callback(hObject, eventdata, handles)
onemirror()
```

```
%%reflect
function [point,vecr,cancel] = reflect(veci,a,fx,fx2,x)
cancel=0;
const=-(veci(2,1)/veci(1,1))*a(1,1)+a(2,1);
if abs(const)==inf
    F1=a(1,1);
    F2=a(1,1);
else

    f=(veci(2,1)/veci(1,1))*x+const;

    F1=double(solve(f));

    F2=double(solve(f-fx,x));
    if fx2 ~= 0
        fxsol=(1:2);
        fysol=(1:2);
        fxsol(1) = double(solve(f-fx,x));
        fysol(1) = subs(fx,x,fxsol(1));
        fxsol(2) = double(solve(f-fx2,x));
```

```
            fysol(2) = subs(fx2,x,fxsol(2));

            tipx = solve(fx2-fx,x);
            tipy = subs(fx,x,tipx);
            if fysol(2)>0 && fysol(2)< tipy
                F2 = fxsol(2);
                fx = fx2;
            elseif fysol(1)>0 && fysol(1) < tipy
                F2 = fxsol(1);

            end

        end

end

if a(1,1)<0 || a(1,1)>10
        cancel=1;
elseif isempty(F2)==1
        cancel=1;
```

```
elseif a(2,1)==0
    Y=subs(fx,x,F2);
    n=Y>0;
    F2=max(F2.*(n));
    if isempty(F2)==1 || F2==0
        cancel=1;
    else
        X=F2;
        Y=max(Y.*n);
        orientation=1;
    end
else
    k1=F2<(a(1,1)-0.01);
    k2=F2>(a(1,1)+0.01);
    X=F2.*(k1+k2);
    if sum(X)<0
        X=min(X);
    elseif sum(X)>0
        X=max(X);
    else
```

```
        X=0;
    end
    if X==0
        Y=0;
    else
        Y=subs(fx,x,X);
    end
    if Y > 0 && Y < tipy
        orientation=1;
    elseif isempty(F1)&& length(F2)==1
        cancel=1;
    else
        X=F1;
        Y=0;
        orientation=0;
    end
end
if cancel==1
    point=a;
    vecr=veci;
```

```
elseif orientation==0
    vecr=[veci(1,1);-veci(2,1)];
    point=[X;Y];
else
    df=dfunc(X,fx);
    point=[X;Y];
    vecdf=[1;df];
    theta=-2*acos(dot(veci,vecdf)/(norm(veci)*norm(vecdf)));
    Id=[cos(theta) -sin(theta);sin(theta) cos(theta)];
    vecr=Id*veci;
end
clear('X','Y','const','df','f','fx','orientation','theta','vecdf','veci','df','vecn','x','m','n','w','F1','F2
','Id','a','k');
end

%%one mirror
function [] = onemirror()
load('arcAngle','arcAngle');
load('gapHeight','gapHeight');
b = gapHeight;
```

```
theta = arcAngle*pi/180;

m = -tan(theta);

syms x

fx = m*x + b;

fx2 = 0;

save previewD

fprintf('variables saved\n');

end


%%function for the top mirror is fx

function [fx] = gapfx(thetat,L,gap,tilt,frac,x,X,b,c)

fx=-sqrt((1/c)*(x)^2);

df5=abs(simplify(dfunc(L/3,fx)));

C=max(double(solve(tan(thetat)-df5,c)));

fx=subs(fx,x,X);

fx=subs(fx,c,C);

%%for tilt

if tilt~=0

    fx=sin(tilt)*X+cos(tilt)*fx;

end
```

```
%%makes the upper mirror intersect with the lower mirror.x=0 y=gap
fx=subs(fx,X,frac-x)+b;
B=solve(subs(fx,x,0)-gap,b);
fx=subs(fx,b,B);
fx1=subs(fx,x,L);
f1=fx1-gap;
C3=-subs(f1,frac,0);
C1=(C3/L);
frac1=(-gap+L*C1)/(2*C1);
fx=subs(fx,frac,frac1);
end

%%two line function
function [] = twoLines()
load('arcAngle1','arcAngle1')
load('arcAngle2','arcAngle2')
load('mirrorLength','mirrorLength')
load('gapHeight','gapHeight')
m1 = tan(arcAngle1*pi/180);
```

```
b = gapHeight;
m2 = -tan(arcAngle2*pi/180);
xintersect = mirrorLength;
syms x
fx = m1*x+b;
yintersect = -m2*mirrorLength;
fx2 = m2*x+yintersect;
save previewD
fprintf('variables saved\n')

%%ComputeReflection
function [] = ComputeReflections()
load('lightAngle','lightAngle')
load('previewD','fx','fx2')
syms x
thetai = lightAngle*pi/180;
interval = 0; fvec = 0; xf = 0; thetat = 1;
for n=1:length(thetat)
        for i=1:length(thetai)
        [number,vecx,vecy]=Reflection(fx(n),fx2,x,thetai(i));
```

```
        if number==2
            fprintf('WARNING: Ray starts at origin, if this is not covered by top mirror the
number of reflections will be zero.');
        end
        end
end
save computeD
fprintf('Calculations Complete\n');
if vecx(length(vecx)-1) >=10
        fprintf('WARNING: Light has escaped the open mirror\n');
end
end
end


%%tent mirror
function [] = tentMirror()
load('arcAngle','arcAngle')
load('mirrorLength','mirrorLength')
load('gapHeight','gapHeight')
load('mirrorTilt','mirrorTilt')
```

```
thetat = arcAngle*pi/180;

L = mirrorLength;

gap = gapHeight;

tilt = mirrorTilt*pi/180;

syms x X y b c frac

fx=gapfx(thetat,L,gap,tilt,frac,x,X,b,c);

save previewD

fprintf('variables saved\n');

end


%%reflection

function [number,vecx,vecy] = Reflection(fx,fx2,x,thetai)

a=[0;0];

n=1;

vecx(1)=0;

vecy(1)=0;

m=tan(pi/2-thetai);

veci=[1;m];

cancel=0;

while cancel==0
```

```
    n=n+1;
    [b,veci,cancel]=reflect(veci,a,fx,fx2,x);
    vecx(n)=b(1,1);
    vecy(n)=b(2,1);
    a=b;
end
number=sum(vecy==0);
end
%%dfunction
function [df]=dfunc(X,fx)
syms x
df=diff(fx);
df=subs(df,x,X);
end
```